

2010

## Through-Steel Power Transmission Using Piezoelectric Transducers

Jr. Phillip Hobson  
*North Carolina Agricultural and Technical State University*

Follow this and additional works at: <https://digital.library.ncat.edu/theses>

---

### Recommended Citation

Hobson, Jr. Phillip, "Through-Steel Power Transmission Using Piezoelectric Transducers" (2010). *Theses*. 27.  
<https://digital.library.ncat.edu/theses/27>

This Thesis is brought to you for free and open access by the Electronic Theses and Dissertations at Aggie Digital Collections and Scholarship. It has been accepted for inclusion in Theses by an authorized administrator of Aggie Digital Collections and Scholarship. For more information, please contact [iyanna@ncat.edu](mailto:iyanna@ncat.edu).

# THROUGH-STEEL POWER TRANSMISSION USING PIEZOELECTRIC TRANSDUCERS

by

Phillip Matthew Hobson, Jr.

A thesis submitted to the graduate faculty  
In fulfillment of the requirements for the degree of  
MASTER OF SCIENCE

Department: Electrical & Computer Engineering  
Major: Electrical Engineering  
Major Professor: Dr. Numan S. Dogan

North Carolina A&T State University  
Greensboro, North Carolina  
2010

School of Graduate Studies  
North Carolina Agricultural and Technical State University

This is to certify that the Master's Thesis of

Phillip Matthew Hobson, Jr.

has met the thesis requirements of  
North Carolina Agricultural and Technical State University

Greensboro, North Carolina  
2010

Approved by:

---

Dr. Numan S. Dogan  
Major Professor

---

Dr. M. U. Bikdash  
Committee Member

---

Dr. John C. Kelly  
Committee Member  
Department Chairperson

---

Dr. Alan Letton  
Interim Associate Vice Chancellor for  
Research and Graduate Dean

# COPYRIGHT

Copyright © 2010

Phillip Matthew Hobson, Jr.

All Rights Reserved

## DEDICATION

To my family. Thank you all for your love, support, and encouragement.

## BIOGRAPHICAL SKETCH

Phillip Matthew Hobson, Jr. was born on September 29, 1979, in Greensboro, North Carolina. He received his Bachelor of Science in Electrical Engineering from North Carolina Agricultural and Technical State University in 2006, and is currently a candidate for the Master of Science degree in Electrical Engineering.

## ACKNOWLEDGMENTS

Many thanks must go to my parents, Phil and Sharon Hobson, for their support of my educational endeavors; especially when I was trying to discover just what it was that I was meant to do in life. Trying to find that one thing to really go after and invest in was difficult for someone with many hobbies and interests. Growing up, I never imagined that I would become an electrical engineer, but looking back, it all seems to make sense. Thanks for always pointing me in the right direction; and a special thanks to my mom, who managed to run a business at home while homeschooling my sister and me. I am so thankful for those years.

Thanks also to my advisor Dr. Numan Dogan who worked diligently and patiently with me through my years as a Graduate student; both in class work and in research, project work, and throughout the thesis writing process. I'm grateful for your extensive knowledge, patience, and good sense of humor!

I would also like to thank Dr. John Kelly and Dr. Marwan Bikdash for their dedication to excellence in teaching and individual contributions to my educational success.

Finally, I would like to thank my wife, Amy, and our daughter Kaitlyn Joy for their love, encouragement, and patience throughout these busy months filled with seemingly infinite hours of work and school. There's nothing harder than being away from the ones that you love. Thanks for always knowing where my heart was at, for inspiring me to do my best, and for filling my life with endless happiness.

## TABLE OF CONTENTS

LIST OF FIGURES .....	ix
LIST OF TABLES .....	xi
LIST OF SYMBOLS .....	xii
ABSTRACT .....	xiv
CHAPTER 1 INTRODUCTION .....	1
<b>1.1 Potential Power Sources</b> .....	1
<b>1.2 Battery Power</b> .....	2
<b>1.3 Vibration Energy Harvesting</b> .....	3
<b>1.4 Wireless Power Transfer</b> .....	4
<b>1.5 Acoustically-Coupled Power Transfer</b> .....	6
CHAPTER 2 SYSTEM DESIGN AND ANALYSIS .....	9
<b>2.1 System Design and Components</b> .....	10
<b>2.2 Initial Calculations</b> .....	16
<b>2.3 Resonant Frequency</b> .....	17
<b>2.4 Power Efficiency</b> .....	30
CHAPTER 3 EXPERIMENTATION AND RESULTS .....	32
<b>3.1 Bracket Assembly</b> .....	32
<b>3.2 Epoxy Bonding</b> .....	35
<b>3.3 Testing Procedure and Results</b> .....	39
CHAPTER 4 PROTOTYPE DESIGN .....	44



<b>4.1</b>	<b>Driving Circuit</b> .....	44
<b>4.2</b>	<b>Receiving Circuit</b> .....	50
CHAPTER 5 CONCLUSIONS .....		52
REFERENCES .....		55
APPENDIX 1 SILICON LABORATORIES C8051F120 CODE LISTING .....		57
APPENDIX 2 TCL/TK GUI CODE LISTING.....		62

## LIST OF FIGURES

<b>FIGURES</b>	<b>PAGE</b>
1.1 - Power-through-steel system overview .....	5
1.2 - Transducer .....	7
2.1 - Transducer Datasheet .....	14
2.2 - Prototype mounting fixture .....	16
2.3 - Transducer impedance versus frequency .....	18
2.4 - Transducer current phase and equivalent circuit .....	19
2.5 - Transducer Anatomy .....	22
2.6 - Transducer component wavelengths.....	24
2.7 - Transducer-to-transducer coupling .....	25
2.8 - Combined transducer model .....	26
2.9 - Transducers epoxied to HY100 steel plate.....	28
2.10 - Combined transducer / HY100 steel model.....	29
3.1 - Transducer test circuit .....	33
3.2 - Transmitting Transducer.....	36
3.3 - Receiving Transducers .....	37
3.4 - Clamped in the vise .....	37
3.5 - Basic test setup.....	38
3.6 - Square wave driving signal, sinusoidal output signal .....	42
3.7 - Sinusoidal driving signal, sinusoidal output signal.....	42

4.1 - Level shifter circuit .....	46
4.2 - PAD113 op amp circuit .....	48
4.3 - PAD113 power op amp .....	48
4.4 - $\pm 95$ power supply output wiring schematic.....	49
4.5 - GUI .....	50

## LIST OF TABLES

<b>TABLES</b>	<b>PAGE</b>
1.1 - Decision matrix of possible power systems .....	2
2.1 - Material properties and acoustic velocities .....	23
2.2 - Material resonant frequencies .....	24
2.3 - Combined transducer resonant frequency .....	27
2.4 - HY100 Steel properties .....	27
2.5 - Combined transducer / HY100 steel resonant frequency .....	29
3.1 - Square wave test using 250-ohm series and 250-ohm load resistances.....	40
3.2 - Sinusoidal wave test using 5-ohm series and 500-ohm load resistances .....	41

## LIST OF SYMBOLS

A	Amps
AC	Alternating Current
c	Acoustic Velocity
COTS	Commercially-available Off-The-Shelf
DC	Direct Current
E	Modulus of Elasticity
e	Efficiency
f	Frequency
$f_R$	Resonant Frequency
g	Gram
GUI	Graphical User Interface
Hz	Hertz
I	Current
kHz	Kilo-Hertz
m	Meter
mm	Milli-meter
N	Newton
P	Power
PC	Personal Computer

PLL	Phase-Locked Loop
PP	Peak-to-Peak
PZT	Lead Zirconate Titanate
R	Resistance
RMS	Root-Mean-Square
S	Second
T	Thickness
UART	Universal Asynchronous Receiver / Transmitter
V	Voltage
VEH	Vibration Energy Harvester
W	Watts
Z	Impedance
$\Lambda$	Wavelength
P	Density

## ABSTRACT

**Hobson, Jr., Phillip Matthew.** THROUGH-STEEL POWER TRANSMISSION USING PIEZOELECTRIC TRANSDUCERS. (**Major Advisor: Dr. Numan S. Dogan**), North Carolina Agricultural and Technical State University.

The objective of this study is to present and define a novel way of transmitting power wirelessly, by use of acoustic waves, through metal using piezoelectric transducers. Piezoelectric ceramic has the characteristic of converting an applied alternating voltage into an associated alternating mechanical movement. At a resonant frequency, efficient power transfer is achieved between opposed mating ultrasonic transducers that are coupled through a separating layer.

Commercially available, off-the-shelf components were used to design a system that produced an amplified square-wave signal that was used to drive an ultrasonic transducer epoxied to a piece of 1/4" thick steel plate. On the opposite side of the steel plate, another ultrasonic transducer was epoxied in the same location as the driving transducer; forming an opposed transducer-steel-transducer configuration. A rectifying circuit was connected to the receiving transducer and the resulting direct current voltage was conditioned using a DC/DC converter to produce a stable voltage to power an electrical load.

Basic test equipment was used to capture signals in order to calculate transmitted and received power, and analysis and experimentation was performed to locate resonant frequencies that produced peak power transfer efficiencies. Power transfer efficiencies of

up to 65% were achieved and over 10 Watts of power were sourced to a resistive test load connected to the output circuit of the receiving transducer. Results of this magnitude represent a significant finding, especially given the low cost and simple design of the system.



# CHAPTER 1

## INTRODUCTION

The goal of the through-steel power transfer project stemmed from the need to have a reliable, safe, power efficient, long-term solution to power an electronic device requiring 10W of power that was to be placed inside of a sealed steel enclosure. Drilling holes in the enclosure was prohibited, thus eliminating the option to supply power to the device via wires from an external power source. Furthermore, batteries were not a viable option either due to several operating constraints; chief among those being the power requirements of the device and the long-term nature of its use, which would require an on-going need to replace or charge batteries. A better option was needed; one that would allow the device to be powered for at least 10 years without human intervention, and that could supply the 10W of power necessary to operate the electronic device.

### **1.1 Potential Power Sources**

At the onset of the project, research was conducted to try to ascertain possible solutions to powering the electronics that were to be sealed inside the steel box. A decision matrix was formed to determine the most ideal system to use among several likely candidates. Table 1.1 outlines the various systems and their respective characteristics that influenced the viability of each candidate for use in this project.

Table 1.1 - Decision matrix of possible power systems

Potential Power System	Pros	Cons	Outcome
Battery	-Easy to implement -Inexpensive	-Must be charged by outside power source -Battery lifespan: may not last 10 years	Not ideal
Energy Harvester	-Potentially easy to implement -“Green” alternative -Provides electrical energy from ambient sources	-Low (~13mW) output power: many harvesters would be needed to provide sufficient power	Not ideal
Acoustically-coupled through wall system	-Uses external power source -Utilizes off-the-shelf components -Easy to implement	-Careful placement of transducers required for most efficient operation -Uses high voltages	Possibility

## 1.2 Battery Power

The first contender that entered consideration for the power system of choice was a battery. With all things being equal, the simplest approach to powering a fairly low power electronic device that was to be installed inside a closed box and remain untouched for a period of about 10 years was to use a battery. This idea was impractical though, as the amp-hour rating of the battery would have to have been impossibly large, about 73000 amp-hours, to meet the power requirements of the system for a period of 10 years. This was simply out of the question. A rechargeable battery could be used, but the necessity of charging would still require power to be delivered somehow to the internals of the sealed box.

### **1.3 Vibration Energy Harvesting**

The next idea that entered consideration as a viable power system candidate was to use an energy harvester mounted inside the box with the electronics. Energy harvesting is an environmentally-friendly “green” concept that has seen a tremendous amount of attention recently, as the resources needed to produce green energy are far less costly and more abundant and renewable than resources needed for traditional energy production. Furthermore, green energy produces none of the noxious emissions and byproducts associated with fossil fuels and other combustible materials typically used to produce power. Going green presented an alluring option for powering the electronics inside of the box. Since the system would remain untouched for an extended period of time, relying on a form of renewable, ambient energy to provide power to the device would be perfect. Green alternatives would present a cost benefit over time, as the upfront funding needed to purchase or develop a means to scavenge ambient energy would be offset by the number of years the harvester would provide free energy to the device.

Sources of ambient energy are plentiful, as reported by Penella et al. [1]. Among the sources of ambient energy available in the environment that the electronics would be located in, only one source appeared a potential option for powering the device: vibration. The environment in which the system would be used was indoors, eliminating the possibility of using either solar or wind energy as a power source. Also, the temperature gradient between the steel wall and the ambient air would be close to zero, eliminating the possibility of using thermal energy harvesting to provide power.

Vibration energy harvesting presented a possibility for use because the local environment where the box would be in use was subject to vibrations induced by motor-driven equipment.

Research was conducted to discover if a commercially-available off-the-shelf (COTS) vibration energy harvester (VEH) was made that could supply enough power to keep the electronic device running, given the amount of available vibration energy present in the walls of the steel box. The idea was to install the VEH to the inside wall of the sealed steel box along with the electronics, thus eliminating the need to have any kind of apparatus external to the box. In effect, the VEH would take the place of the battery, in the previous power system scenario.

At the time of the research, the latest, most advanced offering in VEH technology was a device that could supply 13mW of power indefinitely, given the vibrational forces predicted to be present in the walls of the steel box. To achieve the 10W of continuous power needed to run the electronics, many vibration energy harvesters would have to have been used. Vibration energy harvesters presented an attractive alternative to traditional power production in that a renewable, continuous energy source could be tapped to produce usable power. VEH technology at the time of the research was impractical for use in powering the target electronics though, due to the inherently low power output of the VEH.

#### **1.4 Wireless Power Transfer**

The other possibility examined as a potential candidate for powering the device

was of a novel, but increasingly more interesting nature, given the shortcomings of the previous ideas. This possibility stemmed from the notion of transmitting power through the steel wall; from an external power source to a transmitting transducer connected to the external wall of the box, to a receiving transducer mounted inside the box, thus delivering the transmitted power to the electronics but without the use of wires running through the wall of the box. Figure 1.1 shows a diagram of the proposed system.

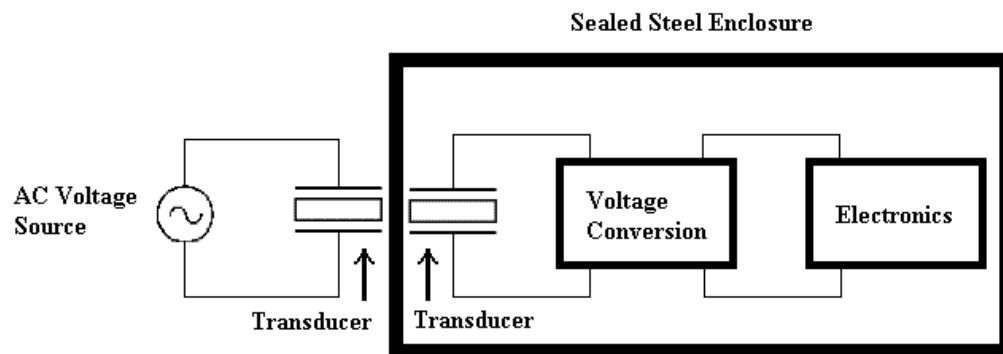


Figure 1.1 – Power-through-steel system overview

In order to couple power from the outside world to the inside of the box, several things would be needed. First would be a source of power, such as a standard 110V AC electrical circuit. Fortunately, 110V AC was an available source of energy at the location in which the steel box was to be used. Needed next was a way to convert the 110V AC power into a signal that would be suitable for driving a piezoelectric transducer to convert electrical energy into acoustic signals in order to transmit power through the steel wall of

the box. On the inside of the box, a receiving transducer would be needed that could take the transmitted acoustic energy and convert it back into electrical power. Also needed would be a way to rectify and regulate the power received on the inside of the box in order to provide a power source that was compatible with the electronics. The output of the power regulator would be connected to the electronics; thus providing power from an external source to the electronics inside the box.

### **1.5 Acoustically-Coupled Power Transfer**

Piezoelectricity is a phenomenon exhibited by certain materials in which an electric potential is generated across a material in response to an applied mechanical force. Conversely, reverse piezoelectricity is the phenomenon where a mechanical deflection is caused in a material by application of an electrical charge across the material. In other words, a piezoelectric material has the ability to convert an applied voltage into a mechanical movement (piezoelectric effect) and a mechanical movement into a voltage (reverse piezoelectric effect). These fundamental characteristics of piezoelectricity made piezoelectric materials a possible candidate for use in developing a through-steel, acoustically-coupled power transfer system.

Research was conducted to gain information into the types of piezoelectric devices and/or materials that would be best suited for use in a power transfer system. Two initial criteria were used as a basis for research into piezoelectric devices. Those criteria were high power handling capability and reliability. Those criteria were based on the 10W power requirement of the load electronics and the fact that the system would

need to remain in use for a period of at least ten years. It was found through research that piezoelectric “sandwich type” transducers, comprised of several layers of piezoelectric material, metal end caps, and a pre-tensioning bolt, had characteristics that made them ideal for use in an acoustically-coupled power transfer system. Transducers of this type are typically used in ultrasonic cleaning devices and are designed to be able to withstand high-power operation and be driven with high-voltage signals. The transducer that was found to be the most ideal for this application was the #90-4070 ultrasonic cleaning transducer manufactured by APC International, Ltd featuring an 80 Watt continuous power handling capability. The #90-4070 piezoelectric transducer was designed to produce a 120 kHz resonant frequency when used in a typical ultrasonic cleaning application where the transducer would be coupled to a tank containing a liquid cleaning solution. The prime reason this device was chosen over other similar transducers was the 80W power-handling capability that this transducer offered. A picture of the transducer is given in Figure 1.2.



Figure 1.2 - Transducer

Power handling capabilities of 30W to 50W were common to most other researched transducers. The additional power capabilities of the APC transducer were attributed to the use of hard lead zirconate titanate (PZT) ceramic in the two piezoelectric elements of the transducer. The use of hard PZT over soft PZT material enabled the transducer to offer more efficient operation due to lower heat generation during continuous operation, higher reliability for long-term continuous use, and greater power handling capabilities. The transducer was manufactured as a commercial off-the-shelf (COTS) component, and thus alleviated the time and expense associated with designing and purchasing a custom component. Three transducers were purchased for lab/prototype use. When the transducers arrived, work began on a prototype through-wall power transfer system.



## CHAPTER 2

### SYSTEM DESIGN AND ANALYSIS

To create an acoustically-coupled power transfer system using piezoelectric transducers, several components would be required; namely, a transmitting transducer and a receiving transducer; both mounted to one wall of the steel box. The transducers would need to be mounted in an “opposed” fashion, with the transmitting transducer mounted on the outside of the steel wall and the receiving transducer mounted on the inside of the steel wall in the same spatial location as the transmitting transducer, as previously shown in Figure 1.1. Mounting the transducers in the same spatial location provides the shortest, most direct signal path from transmitter to receiver and allows the highest power transfer efficiencies to be achieved.

Next, an electrical signal source would be needed to generate a signal in which to drive the transmitting transducer with in order to create a suitable acoustic signal to transmit through the steel. Also needed would be a signal amplifier to provide an adequate level of gain to the driving signal.

On the receiving side of the circuit, the receiving transducer would capture the acoustic waves being driven through the steel via the transmitting transducer and convert them back into an electrical signal. Additional circuitry would be needed to provide rectification, conditioning, and regulation to the received signal such that the voltage and current produced could be made compatible for powering the electronics being used inside of the steel box. For initial test purposes though, the receive electronics were

omitted and a power resistor was used as a load to provide a simple means of measuring received power. Design would begin on the receive electronics after validation had been completed on the design, and efficient operation of the acoustic power transfer system had been realized. A receiving circuit could then be designed and tuned to provide optimal and efficient power regulation given operation of the acoustic system at its most ideal operating point.

## **2.1 System Design and Components**

The overall design of the acoustic power-through-steel system was fairly simple and involved but a few components. The power requirements of the enclosed electronics and predicted power transfer efficiencies of the piezoelectric through-steel power transfer system predicted by Hu et al. [2] drove the design of the transmitting system. Otherwise, the design to provide power to the electronics was nothing more than a simple AC-to-DC converting circuit. In a typical AC-DC electrical circuit, alternating current is rectified and filtered to produce direct current at a particular voltage. The DC voltage is then used to power electronic devices that require direct current, such as a personal computer (PC). The alternating current available for domestic use in North America is regulated to 120  $V_{\text{RMS}}$  with an alternating frequency of 60 Hz. The main difference between an AC-DC converter circuit and the circuit required to drive the piezoelectric transducer is the frequency of the alternating current. Piezoelectric transducers are typically designed to operate at or near their resonant frequency, which is typically at a frequency of 20 kHz or greater; outside the range of human hearing. The resonant frequency of the transducer is

the frequency at which the transducer operates most efficiently and produces peak vibrational and/or electrical output. Given the possibility that 120 V<sub>RMS</sub> may be a suitable voltage level in which to drive the transducer, the 60Hz frequency of the alternating current would be too low to be of benefit. So instead of using AC power directly from a domestic wall outlet, a circuit would have to be devised to allow the frequency, and possibly voltage, of the driving electrical signal to be altered in order to provide an operating point that would place the transducer pair in resonance.

Therefore, to facilitate design and test flexibility, an electrical driving system was developed based on the use of some common electronic bench equipment. First, a signal source was needed. An Agilent 33220A waveform generator was procured and used to provide a driving signal to the acoustic system. The waveform generator was capable of producing multiple types of periodic signals in the ultrasonic frequency range. Furthermore, the 33220A featured USB, RS-232, and GPIB communications, allowing the possibility of automated testing as described in the 33220A User's Guide [3]. To provide gain to the signal that the 33220A waveform generator would produce, a signal amplifier was needed that could provide sufficient output voltage and current to drive the dynamic load that the transducer pair presented. The Krohn-Hite model 7500 amplifier was found to have capabilities ideally suited for driving piezoelectric transducers. The model 7500 amplifier featured 75W of continuous power available over an operating frequency range of DC to 1 MHz and variable voltage gain from 0 dB to 40 dB, producing up to 200 V<sub>PP</sub> of output voltage. The amplifier also featured low distortion operation; providing less than 0.1% of distortion to the applied signal over the frequency

range of the amplifier. These two pieces of equipment served as the basis for creating electrical signals in which to drive the acoustic through-steel prototype system. The waveform generator was connected to the Krohn-Hite amplifier via a 50 ohm coaxial cable connection and the amplifier was joined to the transducer via a pair of 14-gauge, stranded copper wires. Inserted in series between the amplifier and the driving transducer was a current-sense resistor, used to provide a measurement of the driving current via the voltage difference produced across the resistor. An Agilent multimeter was used on the driving side of the transducer setup to provide measurement capabilities for monitoring and recording driving voltage and current.

On the receiving side of the transducer circuit, power resistors were used to provide a simple resistive load to terminate the received signal. A variety of resistance values were purchased to allow experimentation with impedance matching in order to find and/or verify the most ideal load impedance needed to achieve maximum power transfer. A Fluke multimeter was utilized on the receiving side of the circuit to provide voltage and current measurements related to the received power. Additionally, an HP 54602B oscilloscope was used to observe, measure, and record signals on the driving and receiving sides of the circuit.

The final pieces of the prototype system were the most critical; the transducers and the connection they would make to the piece of steel plate. Careful attention was paid to the selection of the piezoelectric transducers. The power requirements of the electronic load were about 10W. The transducers would need to handle that much power in addition to the power that would be wasted due to inefficiencies in the process of

converting electrical energy into acoustic energy, acoustic energy back into electrical energy, and regulating the output voltage to be compliant with the input demands of the target electronics.

The most significant contributor to inefficiency in the acoustic power transfer system would be the bond that the piezoelectric transducers would make with the steel wall. These two bonds would be the biggest point loss in the path of power transfer. No concrete information was available to give indication of how efficient power transfer would be through a 1/4" steel plate using piezoelectric transducers bonded to the steel other than the theoretical information given by Hu et al. [2]. Therefore, without knowing how much input power would need to be expended in order to produce 10W of usable output power, initial estimations for transducer power rating requirements were at least several times that of the load power requirements.

The APC International, Ltd 80W, 120 kHz "sandwich-type" piezoelectric transducer was an ideal match for the application. This transducer was selected to be used in the prototype power transfer system because it featured sufficient power overhead to prevent possible damage to the transducer due to high input power, and was in the same price range and availability as transducers with lower power ratings. Additionally, this transducer featured a smaller physical size than those of lower power ratings, contributing to a lower profile for the end physical design. The datasheet for the transducer is included in Figure 2.1.



APC International, Ltd.  
 APC Products Division  
 Duck Run, PO Box 180  
 Mackeyville, PA 17750 USA  
 Phone: + 570-726-6961  
 Fax: + 570-726-7466

## 120 KHz Ultrasonic Cleaning Transducers

120KHz/80Watts

Catalogue# 90-4070

### Specifications:

Description:	120 KHz Sandwich Transducer
Operating Frequency:	120 KHz
Capacitance:	3.7 nF
Impedance:	50 max.
Mechanical Q (Qm1):	1000 min.
Power:	80 Watts continuous RMS power 60 Watts RMS large fq sweeping
Coupling Factor (kp):	55 % min.
Major OD:	40 mm
Overall LN:	55 mm
Model:	C-1203840

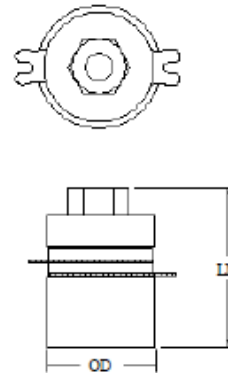


Figure 2.1 - Transducer Datasheet

The 120 kHz natural resonant frequency of the transducer was higher than many other transducers on the market but wasn't necessarily considered a bad trait given the fact that the natural resonant frequency stated in the transducer datasheet was that of the transducer in air – not coupled to anything. Once the transducer pair would be mounted to the steel plate, the resonant frequency of the system would be lowered due mainly to the increased length of the signal path and the speed of sound through the materials employed in the signal path. Of critical importance would be the placement of the

transducers on the steel plate in relation to each other. If the transducers were not placed in near perfect alignment, then power transfer efficiency would suffer greatly, as the attenuation of the ultrasonic signal would increase significantly with the distance of mounting offset between the two transducers. Additionally, the bond that the transducers would make with the steel plate would govern the quality of the signal transfer, as a poor bond would increase acoustic impedance and lower the efficiency of the power transfer.

The final requirement to meet before testing could take place was to mount, or bond, the transducers to the steel plate. Since there was a desire to perform some experimentation with the mounting of the transducers to the steel plate, and given that project resources were limited and only three transducers were purchased, it was decided to devise a mounting fixture that would “press-fit” the transducers to the steel plate instead of permanently bonding them; at least for initial testing. This would allow freedom to experiment with the physical layout of the transducers on the steel plate without running the risk of having to scrap the steel and the transducers if something didn’t turn out quite right. A test fixture was devised using structural lumber to hold the 1’ x 1’ x 1/4” plate of steel in an upright position. To hold the transducers to the steel plate, a clamp fixture was constructed with wood, threaded steel rods, and nuts, and was used to physically press the two transducers to the piece of steel. Figure 2.2 shows the steel plate in the wooden mounting fixture and the transducer clamp assembly. With the completion of the mounting fixture and clamp assembly, initial testing was ready to take place with the prototype acoustic power transfer system.

Figure 2.2 – Prototype mounting fixture

## **2.2 Initial Calculations**

Before testing could begin, some fundamental mathematical guidelines were needed in order to gain a better understanding of the phenomena at work to make the system achieve efficient transfer of power. It was known through the findings of Hu et al. [2] that through-steel power transfer using piezoelectric material was possible. The use of piezoelectric transducers in ultrasonic cleaners was proof of their ability to effectively convert electrical signals into acoustic waves and couple those waves to a medium. This system was a little different from those however, and would need its own analysis. As with any electrical circuit, a series of equations was needed to provide characterization of the devices and components used in the circuit in order to gain a better



understanding of the limitations of the system, what type of input to provide, and what kind of output to expect. Unfortunately, detailed analysis of the piezoelectric devices and the complexities of the boundary conditions created when the transducers are coupled to anything is an inherently mechanical challenge that is ideally suited to the use of finite element analysis, which was outside the scope of this research to tackle. However, system characterization via properties of materials studies were more than adequate to begin the investigation and provided a simpler means to the information necessary to begin testing.

### **2.3 Resonant Frequency**

Upon request, APC International supplied information additional to that of the basic datasheet provided in Figure 2.1. The additional information included impedance versus frequency plots for the model #90-4070 transducer and an equivalent electrical circuit based on the test data gathered while characterizing the transducer with an HP 4194A Impedance/Gain-Phase Analyzer. The impedance versus frequency plot given in Figure 2.3 shows several resonant peaks around 34 kHz, 81 kHz, and 122 kHz, with the peak at ~122 kHz resulting in the greatest drop of impedance, and hence frequency of greatest resonance in free air. Additionally, Figure 2.3 provides a zoomed-in image of the fundamental resonant and anti-resonant peaks of the transducer in free air. Figure 2.4 shows the equivalent circuit model and component values of the transducer when analyzed with the HP 4194A. Also shown in Figure 2.4 is the phase of the current in relation to voltage in the frequency range around the fundamental resonant frequency.

2-27-2007

#90-4070 (120 KHz 80watts)

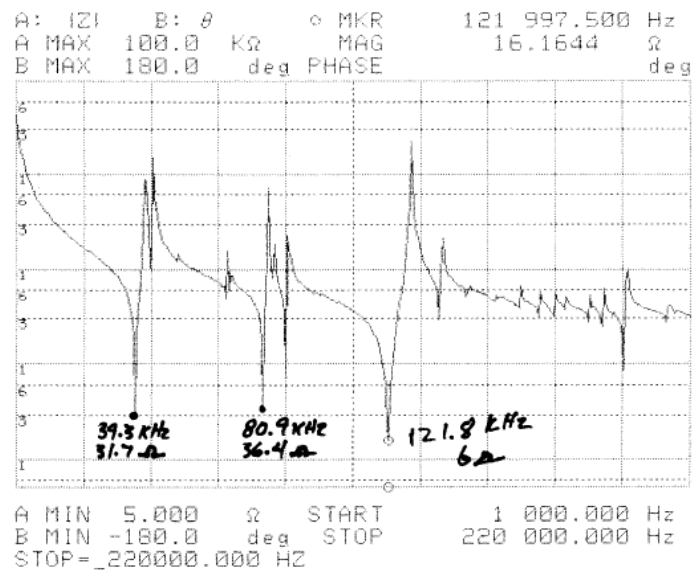
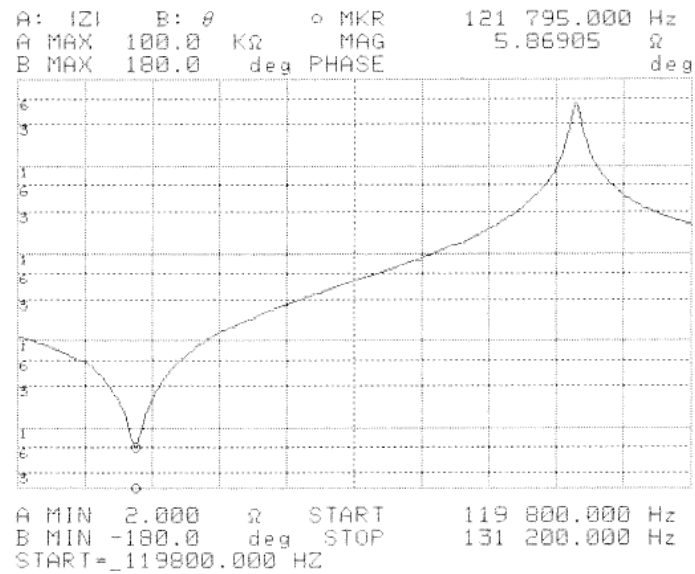
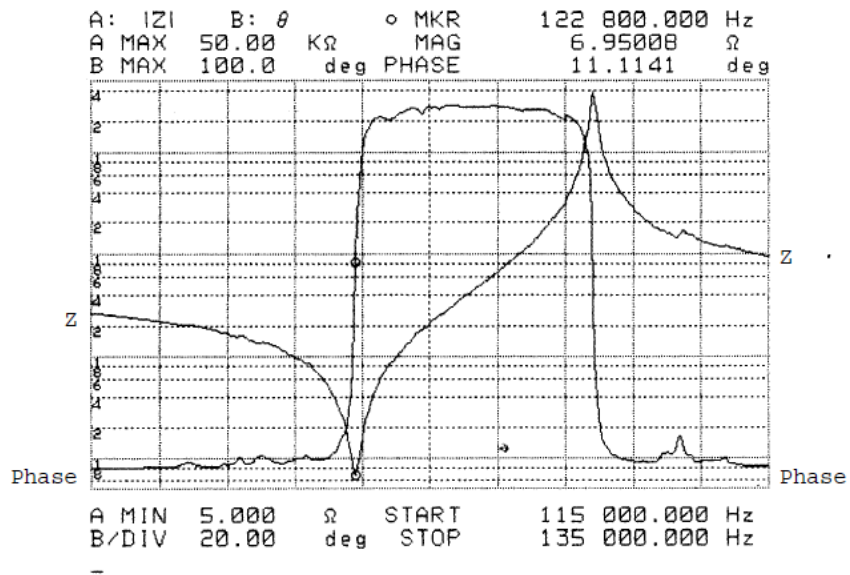


Figure 2.3 – Transducer impedance versus frequency

8/30/2010 JZ

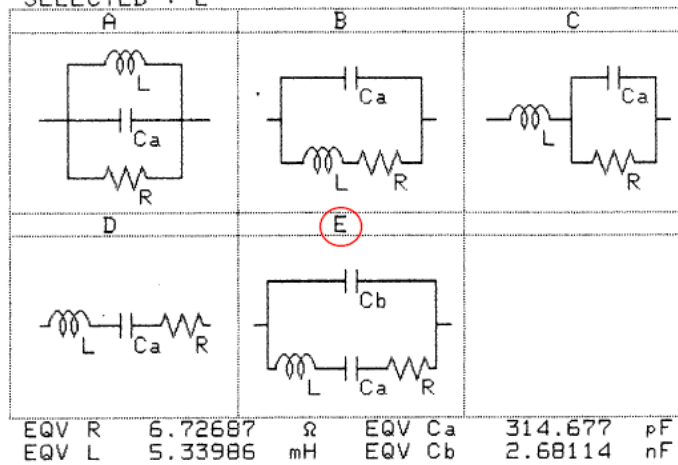
Cat 904070 120KHz80W Sandwich Transducer

Z vs Fq in Air



EQUIVALENT CIRCUIT MODE

SELECTED : E



Equiv Cir "E"

Figure 2.4 – Transducer current phase and equivalent circuit

It can be seen in Figure 2.4 that the phase angle of the current below resonance and above anti-resonance is -90 degrees, indicating that the transducer represents a capacitive load in those frequency ranges. At resonance and anti-resonance, the phase angle is close to zero, signifying the cancellation of inductive and capacitive components and characteristic operation close to that of a resistor. Between resonance and anti-resonance, the transducer is characterized by its inductance, as made evident by the +90 degree current phase angle.

The “free air” resonant frequency is the resonance that the transducer achieves when coupled to nothing – it is the frequency with which the transducer naturally achieves resonance. Resonance is achieved when the transducer is driven at a frequency that causes its intrinsic inductance and capacitance to effectively cancel each other, leaving only a resistive component in the electrical path of the transducer, hence making the transducer appear as a resistive load. The characteristic resistance of the transducer is smallest at the point of fundamental resonance, thus the impedance versus frequency plot shows the lowest impedance at around 122 kHz.

The frequency with which the transducer achieves resonance is based on the physical design of the transducer, and specifically, the thicknesses and acoustic velocities of the PZT ceramic and metal end-caps used in the construction of the transducer. The #90-4070 is a half-wavelength transducer, meaning that each element of the transducer is designed and dimensioned such that the thickness of the element is equivalent to half the wavelength of the resonant frequency, based on the speed of sound in that element. The smallest unit of length in which resonance can be achieved in any medium is at a length

that is half the wavelength of the resonant frequency. A simple example is a rubber band fixed at two points; when plucked, the rubber band oscillates in a half-wave pattern at a fixed frequency. In the same way, the transducer operates in resonance when the thicknesses of the components used are equal to  $\frac{1}{2}$  the length of the resonant frequency wavelength. To give proof, or at least verification, of the design of the transducer for resonant operation at 120 kHz, simple analysis is needed.

The first goal in the analysis is to determine the speed of sound, or acoustic velocity, in each of the materials used in the transducer. The #90-4070 transducer is made of a stainless steel end cap, two layers of APC 880 PZT material with copper electrodes connected, an aluminum face cap, and a pre-tensioning bolt that is used to protect the PZT material of the transducer from breaking during high-power operation. The pre-tensioning bolt runs practically the entire length of the transducer, with the head of the bolt countersunk into the stainless steel end cap and the threaded end terminated in the aluminum face cap of the transducer. The bolt flexes with the vibrational movement of the PZT material, has a negligible effect on resonance, and can be ignored for the sake of analysis. In addition, the copper electrodes connected to the two layers of PZT material are sufficiently thin, measuring about 100 $\mu$ m each, to be ignored for the sake of analysis. Figure 2.5 shows the anatomy of the transducer with thickness measurements of each of the major components of the transducer given. The total length of the transducer is 55mm as shown in Figure 2.1.

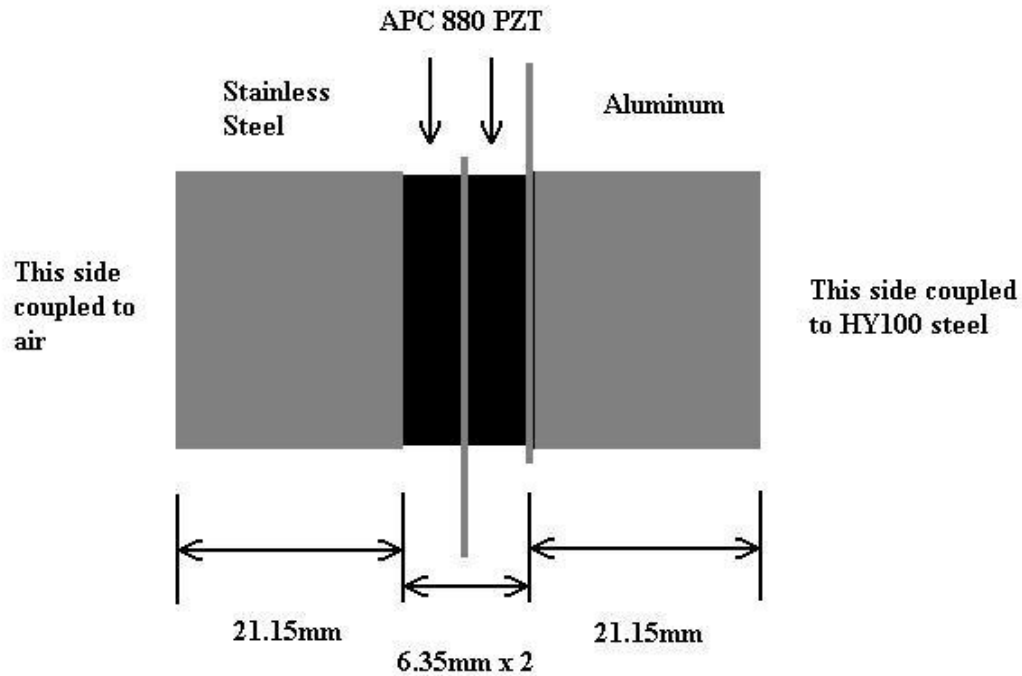


Figure 2.5 - Transducer Anatomy

Both the stainless steel end cap and the aluminum face cap have thicknesses of 21.15mm, whereas the two PZT layers measure 6.35mm each. The acoustic velocity for a material is given by

$$c = \sqrt{(E/\rho)} \quad (2.1)$$

where  $E$  is the modulus of elasticity, and  $\rho$  is the density of the material. Table 2.1 gives the material properties and the computed acoustic velocities for each of the three major materials used in the construction of the transducer.

Table 2.1 - Material properties and acoustic velocities

Material	E (N/m <sup>2</sup> )	$\rho$ (g/m <sup>3</sup> )	c (m/s)
Stainless Steel	$1.96 \times 10^{11}$	$7.81 \times 10^3$	5009.59
PZT 880	$7.20 \times 10^{10}$	$7.60 \times 10^3$	3077.94
Aluminum	$6.80 \times 10^{10}$	$2.70 \times 10^3$	5018.48

Wavelength,  $\lambda$ , can be computed by dividing acoustic velocity by frequency,  $f$ .

$$\lambda = c / f \quad (2.2)$$

Since the nominal resonant frequency of the transducer in air is known to be 120 kHz, the wavelength in PZT 880 material at the resonant frequency is

$$\lambda = 3077.94 / 120000 = 25.6 \text{ mm}. \quad (2.3)$$

It is also known that the transducer is designed as a “half-wavelength” device, as is common in devices designed to operate at resonance since a half-wavelength represents the smallest unit in which resonance can be achieved. Therefore, the theoretical thickness of the PZT 880 material in the transducer should be

$$\lambda / 2 = 12.8 \text{ mm} \quad (2.4)$$

This agrees with the actual thickness of the PZT material within 1%, as the transducer features two PZT disks that are 6.35mm in thickness each, measuring a total thickness of 12.7mm. Therefore, it is evident that the resonant frequency,  $f_R$ , of the materials used in the design of the transducer is given by

$$f_R = c / \lambda = c / (2 * T), \quad (2.5)$$

where  $T$  is the thickness of the material in meters. Using equation 2.5, the resonant frequencies of the materials can be computed and are presented in Table 2.2.

Table 2.2 - Material resonant frequencies

<b>Material</b>	<b><math>c</math> (m/s)</b>	<b><math>T</math> (m)</b>	<b><math>f_R</math> (Hz)</b>
Stainless Steel	5009.59	0.02115	118430.02
PZT 880	3077.94	0.01270	121178.74
Aluminum	5018.48	0.02115	118640.19

All of the material resonant frequencies are within 1.5% of the nominal resonant frequency of 120 kHz. This proves that the individual components used to make the transducer have to be specifically tuned to the same frequency as the desired resonant frequency of the transducer. The transducer therefore is a combination of components that are dimensioned in lengths of  $\frac{1}{2}$  the wavelength of the desired transducer resonant frequency, based on the physical properties of the materials used, as shown in Figure 2.6.

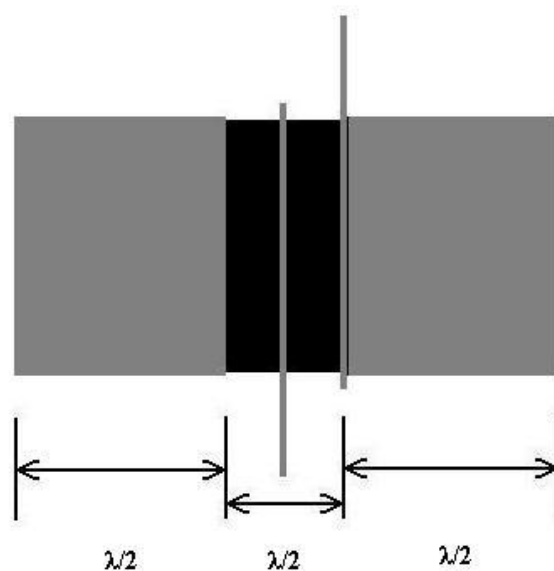


Figure 2.6 - Transducer component wavelengths



Material properties information can therefore be used to determine the resonant frequency of the through-steel power transfer system consisting of one driving transducer and one receiving transducer, with a HY100 steel plate sandwiched in between. Before the steel plate is introduced into the analysis, it's helpful to analyze the characteristics of the transducer pair as if they were coupled to each other. In this case, the face of the driving transducer would be bonded to the face of the receiving transducer as shown in Figure 2.7.

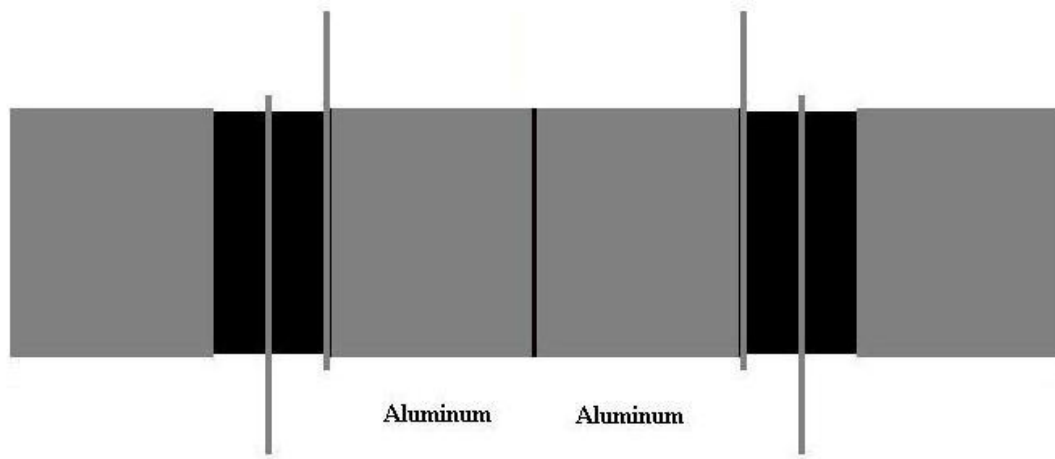


Figure 2.7 - Transducer-to-transducer coupling

This model differs from that of the “free air” transducer model in that one transducer is meant to drive the other instead of each transducer operating in free air and resonating with its own vibrational movement. As such, the resonant frequency will be altered because the length of the signal path is doubled from that of a single transducer. The

driving signal will travel twice the distance as that of the single transducer before it is reflected back to the driving PZT. To simplify the analysis of the joined transducer model, identical components of the transducers can be combined to form a single, large transducer which can be analyzed using the same approach as that of the previous free air transducer. Figure 2.8 depicts the combined transducer model.

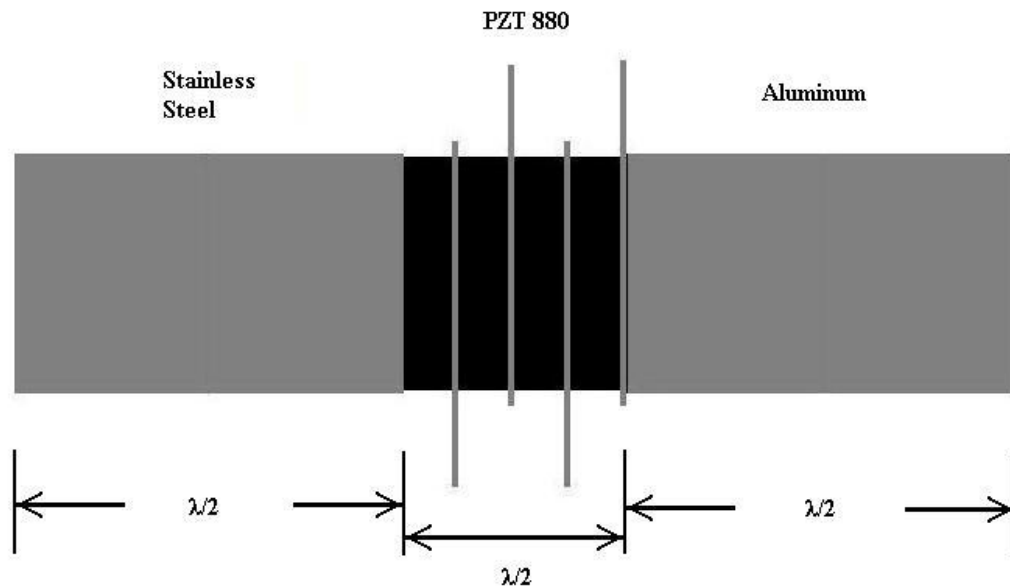


Figure 2.8 - Combined transducer model

When the combined transducer model is analyzed in the same manner as the single transducer, it is revealed that the resonant frequencies of the components in the combined transducer model are effectively halved due to the doubling of the component thicknesses as shown in Table 2.3.

Table 2.3 - Combined transducer resonant frequency

<b>Material</b>	<b><math>C</math> (m/s)</b>	<b><math>T</math> (m)</b>	<b><math>f_R</math> (Hz)</b>
Stainless Steel	5009.59	0.0423	59215.01
PZT 880	3077.94	0.0254	60589.37
Aluminum	5018.48	0.0423	59320.09

Combining the elements of the transducers in this way is analogous to combining passive electrical circuit elements to form a simplified circuit model.

The final step in determining the resonant frequency of the through-steel system is to include the HY100 steel plate in the analysis. The thickness of the steel plate is  $\frac{1}{4}$ ", or 6.35mm. The material properties of the HY100 steel are given in Table 2.4.

Table 2.4 - HY100 Steel properties

<b>Material</b>	<b><math>E</math> (N/m<sup>2</sup>)</b>	<b><math>\rho</math> (g/m<sup>3</sup>)</b>	<b><math>c</math> (m/s)</b>	<b><math>T</math> (m)</b>	<b><math>f_R</math> (Hz)</b>
HY100 Steel	2.05E+11	7.87E+03	5103.75	0.00635	401870.24

The resonant frequency of the steel plate is much higher than that of the transducers, indicating that the steel plate would remain relatively unaffected by the resonant operation of the attached transducers. The steel plate would however, add to the length of the signal path that the acoustic wave would travel through in order to propagate from the driving transducer to the receiving transducer. Figure 2.9 shows the arrangement of the transducers to the steel plate. The aluminum face caps of each transducer are epoxied to the HY100 surface. The addition of the steel plate adds complexity to the analysis of the system. The steel isn't dimensioned to represent a half-

wavelength signal path, but is sufficiently thin to be modeled as an addition to the thicknesses of the end and face caps of the combined transducer in Figure 2.8.

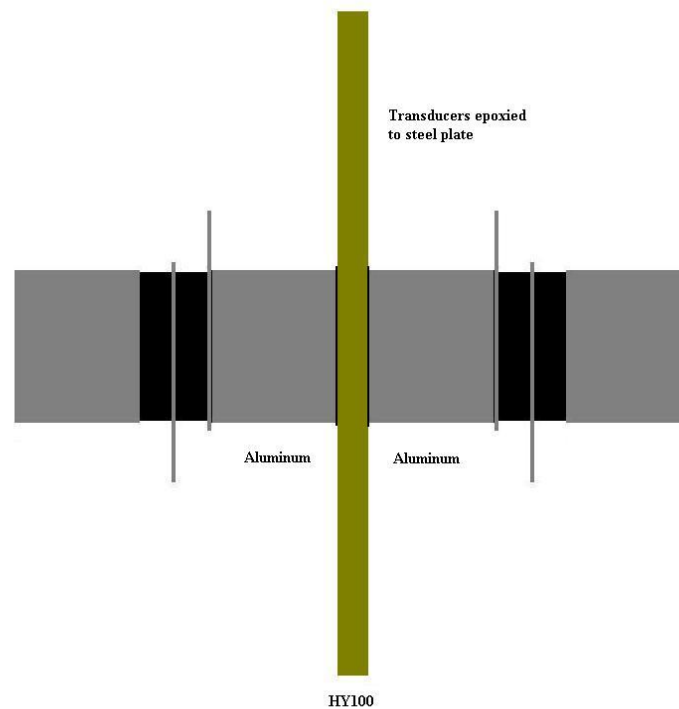


Figure 2.9 - Transducers epoxied to HY100 steel plate

Modeling the HY100 steel thickness as an integral part of the transducer end and face caps will make the resonant frequencies of the metals lower than that of the PZT material. The lower resonance governs the overall resonant frequency of the power-through-steel system, as the increased length in the signal path yields an increase in the amount of time needed for the signal to propagate from the driving transducer to the receiving transducer and back. Following the procedure of analysis for the combined transducer model, the

combined transducer/steel plate model is given in Figure 2.10. Using the combined transducer / steel plate model yields a resonant frequency of ~55 kHz for the lowest resonant frequency component of the system as shown in Table 2.5.

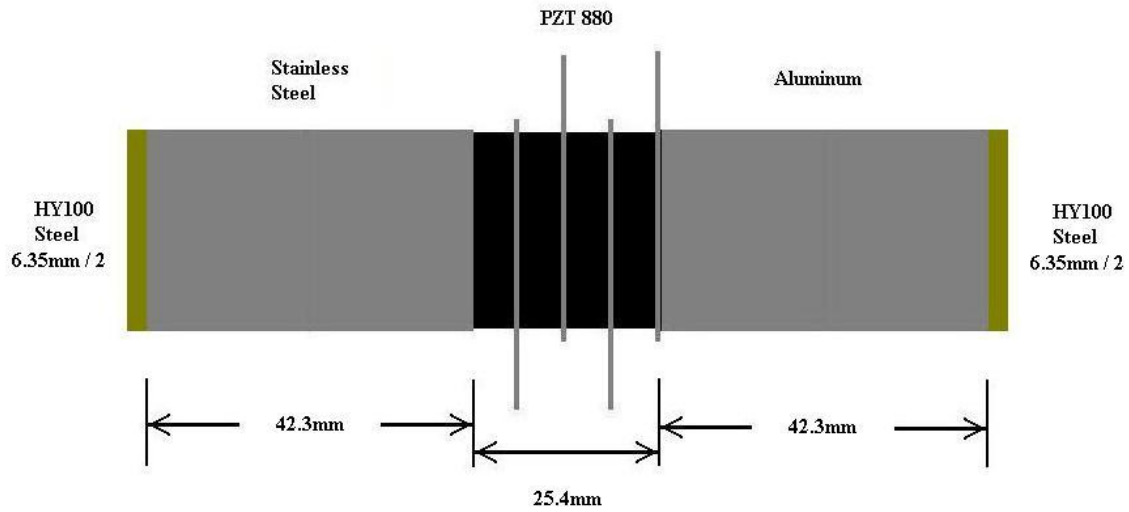


Figure 2.10 - Combined transducer / HY100 steel model

Table 2.5 - Combined transducer / HY100 steel resonant frequency

Material	$c$ (m/s)	$T$ (m)	$f_R$ (Hz)
Stainless Steel + HY100	5009.59	0.045475	55080.70
PZT 880	3077.94	0.025400	60589.37
Aluminum + HY100	5018.48	0.045475	55178.45

The thickness,  $T$ , for the stainless steel and aluminum transducer caps combines the thickness of each cap from the combined transducer model, 42.3mm, with half the thickness of the HY100 steel plate, 3.175mm, since the HY100 was split equally among each side of the transducer in the equivalent model. Also, the acoustic velocity of HY100

steel is nearly 100m/s faster than that of either stainless steel or aluminum, but the difference was considered insignificant for the sake of model simplicity.

The result of the resonant frequency analysis concludes that the through-steel power transfer system should be able to operate in resonance at a frequency close to 55 kHz. There is a margin for variation though, as the model and analysis don't take into consideration one important aspect; the quality of the bond that the transducers would make with the HY100 steel. This model assumes a perfect bond between the components and doesn't make provisions for imperfections in the coupling of the transducers to the steel plate. Given that the transducers would ultimately be bonded to the steel plate with epoxy, it would be expected to have, at a minimum, imperfections in the bonding of the two transducers that would lead to an additional drop in the resonant frequency of the overall system. The amount of the drop would be determined by the quality of the epoxy bond, and as such is impossible to predict reliably. The computed resonant frequency serves as a guideline to aid testing and help to provide understanding of the operation and dynamics of the system.

## **2.4 Power Efficiency**

Needed next would be a way to compute the power transfer efficiency expected from the through-steel transfer system. According to APC International [4], transfer efficiency could be predicted by the value of the transducer thickness-mode electromechanical coupling factor,  $k_{33}$ , which for APC 880 PZT was 0.62. The value of  $k_{33}$  is not in and of itself a true representation of the transfer efficiency to be expected in

the through-steel transfer system, as it doesn't account for dielectric losses or mechanical losses that could be present in the construction of the transducers or in the bonding with which they make to the HY100 plate. It is an indicator though, of the effectiveness with which the PZT material converts electrical energy into mechanical energy and vice versa. The true measure of efficiency is the ratio of converted useable power delivered to the test load to the total power delivered to the transducer pair. According to APC International [4], well-designed systems can exhibit efficiencies that exceed 90%. An accurate portrayal of the total efficiency of the system is hard to calculate given the uncertainties afforded by the quality of the bond between the transducers and the steel plate. The value of  $k_{33}$  though, serves as a baseline for estimating an efficiency to be realized in the actual system though, as it states a known value for the efficiency with which the transducer converts energy. Therefore, given that two transducers are used in conjunction, one to convert electrical energy to mechanical energy and the other to convert mechanical energy back to electrical energy, the expected operational efficiency would be given by

$$e = k_{33}^2 = 0.3844, \quad (2.6)$$

where the efficiency,  $e$ , is a product of the electromechanical coupling factors of the two transducers. The input power requirement can then be stated as a function of the necessary output power requirement and the efficiency product.

$$P_{in} = P_{out} / 0.3844 \quad (2.7)$$

Therefore, in order to produce 10W of usable power on the receiving side of the circuit, the driving transducer would need to receive in excess of 26W from the signal amplifier.

## CHAPTER 3

### EXPERIMENTATION AND RESULTS

With a set of equations in place and some expected values in mind, the work of creating a power-through-steel transfer system began. Initial experimentation was performed to discover if through-steel power transfer was indeed possible, and to find out how closely the results of the experimental setup would match those derived analytically.

#### **3.1 Bracket Assembly**

As previously stated and shown in Figure 2.2, a specially devised bracket assembly was used to press-fit the transducers to the steel plate to enable rapid prototyping and testing of the transducers. The bracket was easy to use and allowed for some level of convenience in testing the system. The transducers were aligned to each other and clamped to the steel plate using the devised clamping fixture. Glycerin couplant was used on the mating surfaces of the transducers and steel plate to help achieve a good bond; providing a more efficient power transfer between the components than would otherwise be achieved with just a metal-to-metal connection. The signal generator was programmed to produce a 3 V<sub>PP</sub>, 55 kHz sinusoidal wave and the signal amplifier was configured to provide a gain of 10. The circuit schematic of the test setup is detailed in Figure 3.1.



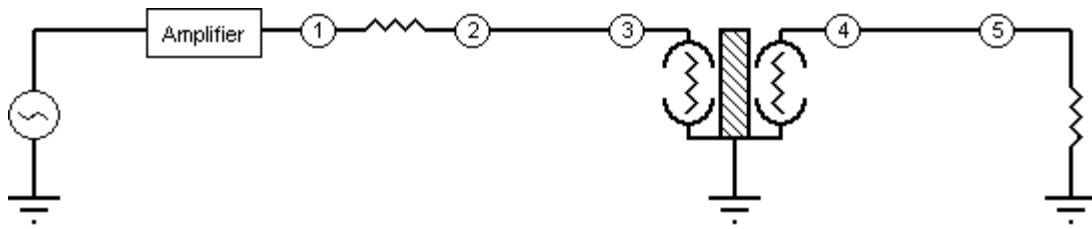


Figure 3.1 - Transducer test circuit

The circuit was fairly simple; only two resistors were used in conjunction with the transducers and test equipment. The first resistor was connected in series between the power amplifier and the driving transducer between points 1 and 2 on the schematic. This resistance was used in conjunction with the measured RMS voltage to calculate the RMS current on the driving side of the circuit.

The receiving side of the circuit was terminated with a load resistance; between point 5 and ground. This was used to simulate the target circuit that the power-through-steel apparatus would energize. For the sake of reliability and more importantly, safety, the steel plate itself was grounded to prevent any build-up of charge that could result in electrical shock.

The oscilloscope was connected to the circuit on both the driving and receiving sides. Channel 1 of the oscilloscope was connected on the driving side of the circuit between point 1 and ground to measure the RMS voltage output of the power amplifier. Once this measurement was taken, the channel 1 lead was removed from point 1 and reconnected between point 2 and ground. This measurement recorded the RMS voltage at the transducer terminal, after the series resistor in the circuit. The series resistance

provided a voltage drop that was used in the calculation of the RMS driving current, and hence, the power delivered to the driving transducer. Equations 3.1 and 3.2 show these calculations.

$$I_{Driving,RMS} = (V_1 - V_2) / R_{Series} \quad (3.1)$$

$$P_{Driving} = I_{Driving,RMS}^2 * R_{Series} \quad (3.2)$$

Channel 2 of the oscilloscope was connected between point 5 and ground on the receiving side of the circuit. This channel measured the RMS voltage delivered to the load by the receiving transducer. The measured received RMS voltage, along with the value of the load resistance was used to calculate the received RMS current and hence, calculate the power delivered through the steel plate. Equations 3.3 and 3.4 show these calculations.

$$I_{Load,RMS} = V_{Load} / R_{Load} \quad (3.3)$$

$$P_{Load} = (I_{Load,RMS})^2 * R_{Load} \quad (3.4)$$

The efficiency of the power transfer through the steel wall was a simple percentage calculation given by Equation 3.5.

$$e = (P_{Load} / P_{Driving}) * 100 \quad (3.5)$$

The signal source and amplifier were started only to find that practically no signal was being produced on the receiving side of the circuit. The driving transducer was receiving the correct signal level as verified by measurement of the signal present at the leads of the transducer. After a short while of troubleshooting, the problem was found. The flexibility in testing that the bracket afforded caused a problem. It was discovered

that the transducers were not being sufficiently secured to the steel plate. During testing, vibrations would cause the transducers to slip very slightly out of alignment, hence yielding unrepeatable and very inefficient results. Measured efficiencies of power transfer were at most, under 10%.

### **3.2 Epoxy Bonding**

To combat the problem and allow the test process to continue, the transducers were permanently mounted to the steel plate using 4-minute structural epoxy. The epoxy bond proved itself to be very reliable and greatly increased the measured power efficiency of the system.

Before the transducers were mounted, the surfaces of the HY100 steel plate were prepped with 150-grit sandpaper and cleaned thoroughly with rubbing alcohol. Next, careful measurement was taken of the steel plate using a rigid steel rule. Layout lines were marked on each side of the plate with a permanent marker. The lines made a crosshatch on each side of the plate, identifying the center point that would be used for positioning the transducers.

Next, the plate was laid flat on a tabletop and the two parts of the epoxy, resin and hardener, were dispensed in equal amounts on the surface of the plate at the center point just marked. The epoxy was carefully and thoroughly mixed, being sure to not create bubbles in the mixture which could lead to inconsistent bond density. Immediately after sufficient mixing, a transducer was placed on top of the epoxy mixture and pressed firmly to the surface of the steel to ensure good bonding. Care was taken not to allow the

transducer to slide out of alignment of the center point. Pressure was applied to the transducer for several minutes to allow enough time for the initial epoxy set before flipping the plate and repeating the process on the other side of the steel. Once both transducers were mounted to the steel plate, the whole apparatus was set aside for several hours to allow the epoxy to cure.

After about 4 hours of cure time, the minimum amount of time required by the epoxy to initially cure, the steel plate was clamped into a small bench vise which was mounted to the surface of a mobile metal instrument cart. All subsequent testing of the power-through-steel was performed using this setup. Figures 3.2, 3.3, and 3.4 show the transducers mounted to both the transmitting and the receiving sides of the steel plate.



Figure 3.2 - Transmitting Transducer

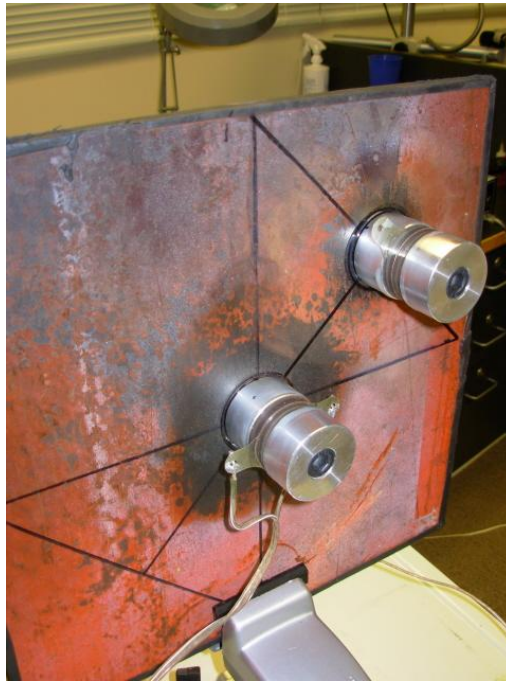


Figure 3.3 - Receiving Transducers



Figure 3.4 - Clamped in the vise

In addition to the center-mounted receiving transducer, the additional transducer was mounted in an offset position to the driving and receiving transducer pair. This offset transducer was epoxied to the steel plate in the same manner as the other two transducers and its purpose was to measure attenuation of the transmitted signal reflections in the steel plate. The offset transducer can be seen in Figure 3.3 and Figure 3.4.

For cabling, 14-gauge stranded copper wire was used to connect transducers to the test equipment. The wire leads were soldered carefully to the terminals of the transducers to eliminate any chatter or noise that could be produced by ultrasonic frequencies on faulty metal interconnects. The steel plate was mounted in a clamp that was fixed to an instrument cart that housed all of the test equipment as shown in Figure 3.5.

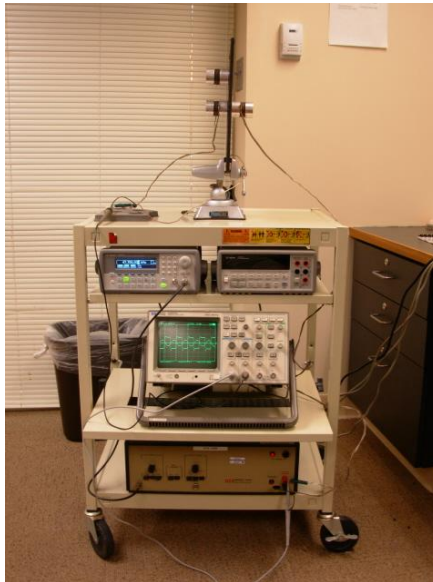


Figure 3.5 - Basic test setup

### 3.3 Testing Procedure and Results

A periodic electrical signal is required to drive the input transducer in order to produce the acoustic energy needed to push the signal through the steel plate. In order to verify the resonant frequency of the transducers/steel plate combination as calculated in chapter 2, a frequency sweep was performed. With the waveform generator programmed to produce a 3 V<sub>PP</sub> square wave signal and the power amplifier adjusted to yield a gain of 10, the square wave frequency was swept from 20 kHz to 200 kHz. A peak resonance was found at 47.7 kHz, yielding a very nice power transfer. This actual resonant frequency as measured in-system was about 13% lower than that of the calculated resonant frequency, 55 kHz. The difference is understandable given the imperfections expected in the bonding between the transducers and the steel plate. The two layers of epoxy between each transducer and the steel plate, though thin, could conceivably lower the acoustic velocity of the signal path, resulting in a lowered system resonant frequency.

Once the resonant frequency was discovered, testing continued using the procedure and test circuit described in section 3.1. Through testing and experimentation, it was discovered that the transducers, mounted with epoxy to the steel plate, could consistently yield power transfer efficiencies of 65%. Further, power handling capabilities of the transducers were quite impressive. Power delivery of 10W to the load resistor was achieved, with no heat dissipation noticed in the transducers. The load resistor was quite hot though, being rated at 12 Watts.

Two different experiments were performed, the first of which being a power transfer efficiency characterization using a square wave signal. The series and load

resistances of the square wave test were both 250 ohms. The second characterization was performed using a sinusoidal signal and utilizing series and load resistances of 5 ohms and 500 ohms, respectively. In both cases, the input signal peak-to-peak voltage amplitude,  $V_{IN,PP}$ , from the waveform generator was swept from 1  $V_{PP}$  to 10  $V_{PP}$ , the amplifier was set to provide a signal gain of 10, and calculations using Equations 3.1 through 3.5 were performed on the resulting test data. The results of two different experiments are given in Table 3.1 and Table 3.2. It is important to note that all values in Table 3.1 and Table 3.2, except for  $V_{IN,PP}$ , are root-mean-square (RMS) values.

Table 3.1 - Square wave test using 250-ohm series and 250-ohm load resistances

$V_{IN,PP}$	$V_{1,RMS}$	$V_{2,RMS}$	$I_{Driving,RMS}$ (A)	$P_{Driving,RMS}$ (W)	$V_{Load,RMS}$	$I_{Load,RMS}$ (A)	$P_{Load,RMS}$ (W)	Efficiency %
1.00	10.200	6.000	0.017	0.101	3.800	0.015	0.058	57.300
2.00	20.250	11.800	0.034	0.399	7.450	0.030	0.222	55.700
3.00	30.700	18.000	0.051	0.914	11.330	0.045	0.513	56.200
4.00	40.900	24.100	0.067	1.620	15.150	0.061	0.918	56.700
5.00	51.200	30.000	0.085	2.544	19.000	0.076	1.444	56.800
6.00	61.500	35.800	0.103	3.680	23.100	0.092	2.130	58.000
7.00	71.800	41.300	0.122	5.040	27.400	0.110	3.000	59.600
8.00	79.100	45.400	0.135	6.120	30.300	0.121	3.670	60.000
9.00	81.500	46.200	0.141	6.520	31.500	0.126	3.970	60.800
10.00	85.000	48.600	0.147	7.150	33.000	0.132	4.356	60.900



Table 3.2 - Sinusoidal wave test using 5-ohm series and 500-ohm load resistances

$V_{IN,PP}$	$V_{1,RMS}$	$V_{2,RMS}$	$I_{Driving,RMS}$ (A)	$P_{Driving,RMS}$ (W)	$V_{Load,RMS}$	$I_{Load,RMS}$ (A)	$P_{Load,RMS}$ (W)	Efficiency %
1.00	7.110	7.027	0.016	0.113	6.180	0.012	0.077	67.564
2.00	14.240	14.070	0.033	0.464	12.400	0.025	0.308	66.326
3.00	21.540	21.290	0.049	1.033	18.790	0.038	0.707	68.442
4.00	28.720	28.370	0.068	1.928	25.120	0.050	1.264	65.569
5.00	35.900	35.460	0.085	3.030	31.550	0.063	1.994	65.825
6.00	43.100	42.580	0.101	4.299	37.900	0.076	2.878	66.935
7.00	50.430	49.800	0.122	6.092	44.460	0.089	3.960	65.006
8.00	57.750	57.060	0.134	7.645	50.950	0.102	5.201	68.029
9.00	64.720	63.920	0.155	9.929	57.090	0.114	6.530	65.762
10.00	70.880	70.010	0.169	11.827	62.200	0.125	7.751	65.537

Figure 3.6 shows a screen shot from the oscilloscope while using a square-wave signal. Channel 1 is measuring the driving transducer RMS voltage and Channel 2 is monitoring the RMS voltage across the resistive load. It can be seen in Figure 3.6 that the slew rate of the square wave is faster than that of the transducer pair. The transducer pair could not convert the electrical excitation into mechanical movement fast enough to keep up with the signal, thus the resulting output of the receiving transducer was a sinusoidal wave.

Figure 3.7 shows a screen shot from the oscilloscope while using a sinusoidal signal. Channel 1 is measuring the driving transducer RMS voltage and Channel 2 is monitoring the load RMS voltage. The load voltage is the smaller of the two signals.

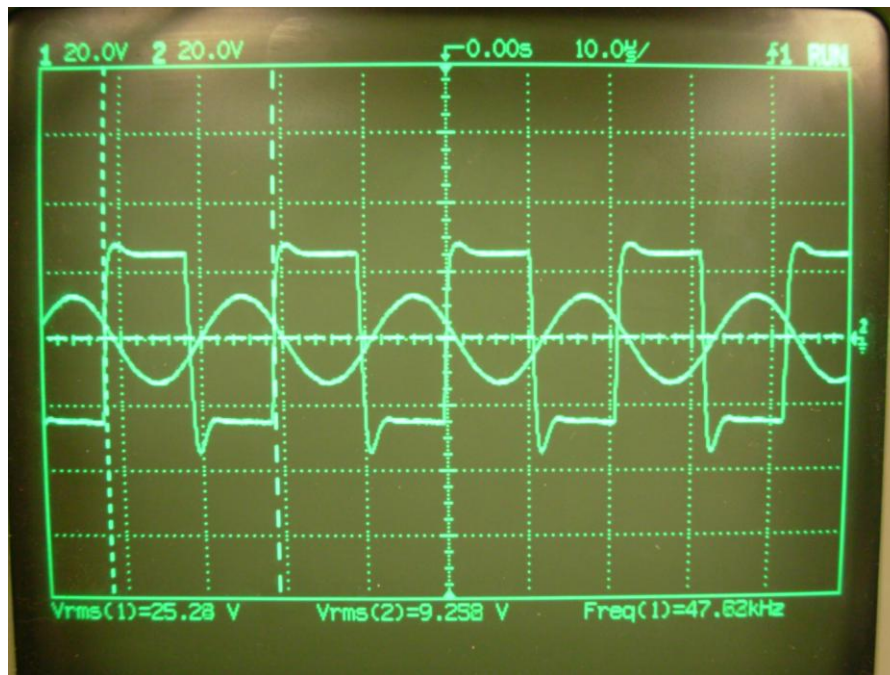


Figure 3.6 - Square wave driving signal, sinusoidal output signal

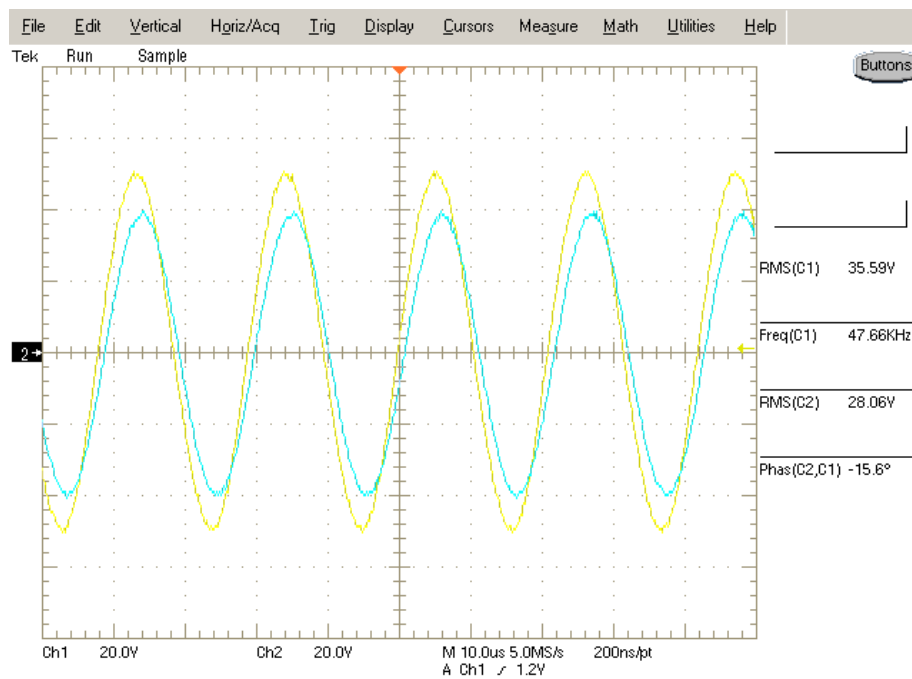


Figure 3.7 - Sinusoidal driving signal, sinusoidal output signal

The test and experimentation proved that power transfer through a steel wall using piezoelectric transducers was indeed possible, and that it was possible to transfer enough power through the steel wall to supply the needs of the electronics that would ultimately be used inside of the sealed box. The transducer-based power-through-steel system worked; and it worked at a greater-than-expected level of efficiency - ~65% efficiency compared to the computed ~38% - which is an added bonus that resulted in less wasted power overhead. The results of the experimentation provided insight into the analysis performed in Chapter 2. The analytical results for resonant frequency proved too high, as the analytical model failed to take into account acoustic impedance that could be introduced into the signal path by the inclusion of the epoxy layers that would serve to couple the transducers to the steel plate. The analytical results for power efficiency were too conservative, as the estimation using the PZT electromechanical coupling factor failed to account for operation of the transducers at resonance which allows the transducers to work synergistically and hence, more efficiently. The analysis results did prove helpful though, as the results provided a baseline for experimentation to be performed upon and suggested that the power through steel transfer was indeed feasible.

## CHAPTER 4

### PROTOTYPE DESIGN

With promising results obtained during test and experimentation, the final step remaining in the implementation of the through-steel power system was to design and build prototype driving and receiving circuits. During test and experimentation, bench instrumentation was used to provide the driving signal to the transducer pair, and a power resistor was used to terminate the signal from the receiving transducer and enable power measurements to be easily taken. For the final system, a more compact, specialized driver was needed that could provide the necessary amplified signal to drive the transducers, and an efficient regulating circuit was needed to convert the sinusoidal output signal of the receiving transducer to a 5 V<sub>DC</sub> level. COTS components were used to implement the required functionality. In addition, open source software was used to design a graphical user interface (GUI) that allowed a user with a PC to change the operating frequency of the signal source, allowing changes to be made to ensure operation at the point of resonance.

#### **4.1 Driving Circuit**

The driving circuit was based on a microcontroller, a MOSFET-based power amplifier, and a power supply. The microcontroller was programmed to output a square-wave signal based on an internal clock. Several approaches to creating a signal source

were available, including using programmable timers or oscillators, but a microcontroller was chosen because of the ease of use it offered in generating precise signals, and for the design flexibility it afforded for implementing computer control of the driving system. The microcontroller chosen for use was a Silicon Laboratories C8051F120 high speed, mixed signal microcontroller. The C8051F120 featured high-speed operation via an internal phase-locked loop (PLL) circuit which was utilized in order to increase the microcontroller's clock frequency to about 100 MHz. The high speed operation was required, at least for the prototype system, to permit small changes to be made in the output clock frequency via command from the host PC. The microcontroller incorporated a universal asynchronous receiver/transmitter (UART), which enabled communication with a host PC. The PC user would issue a command via the UART for the microcontroller to change the frequency of the signal, and the microcontroller would adjust its output signal according to the frequency value given in the command. In the absence of a host PC, the microcontroller would default to operating with a 47.7 kHz square-wave signal. The Silicon Laboratories C8051F120 Datasheet [5] was used as a guide to program the microcontroller. The code for the microcontroller was developed and compiled using the Keil  $\mu$ Vision<sup>®</sup>3 Integrated Development Environment (IDE) software with the aid of the  $\mu$ Vision User's Guide [6]. The code listing for the microcontroller is given in Appendix 1.

The output signal from the microcontroller was a unipolar square wave with voltage levels ranging from 0 V<sub>DC</sub> to 3.3 V<sub>DC</sub>. In order to allow the driving PZT to swing from its most compressed state to its most expanded state, the signal driving the PZT

would need to be bipolar. In order to convert the unipolar signal from the microcontroller into a bipolar signal, a level-shifting circuit was required. The level shifter was comprised of a simple comparator circuit utilizing a Linear Technology LT1017 comparator, with  $+5\text{ V}_{\text{DC}}$  and  $-5\text{ V}_{\text{DC}}$  references. Utilizing the LT1017 datasheet [7], the comparator circuit was biased to  $1.65\text{ V}_{\text{DC}}$ , exactly half of the  $3.3\text{ V}_{\text{DC}}$  input signal, allowing any input voltage greater than  $1.65\text{ V}_{\text{DC}}$  to be output as a positive voltage, and any input voltage less than  $1.65\text{ V}_{\text{DC}}$  to be output as a negative voltage. On the output of the comparator, a potentiometer was used to allow signal gain adjustment. The amplitude of the bipolar signal was adjustable to any value between  $0\text{ V}_{\text{DC}}$  and  $\pm 5\text{ V}_{\text{DC}}$ . The potentiometer output was buffered by a Linear Technology LT1001 op amp configured as a unity buffer using the information given in the LT1001 datasheet [8]. The unity buffer was used to clean the signal from the output of the potentiometer. A schematic of the level shifter is given in Figure 4.1.

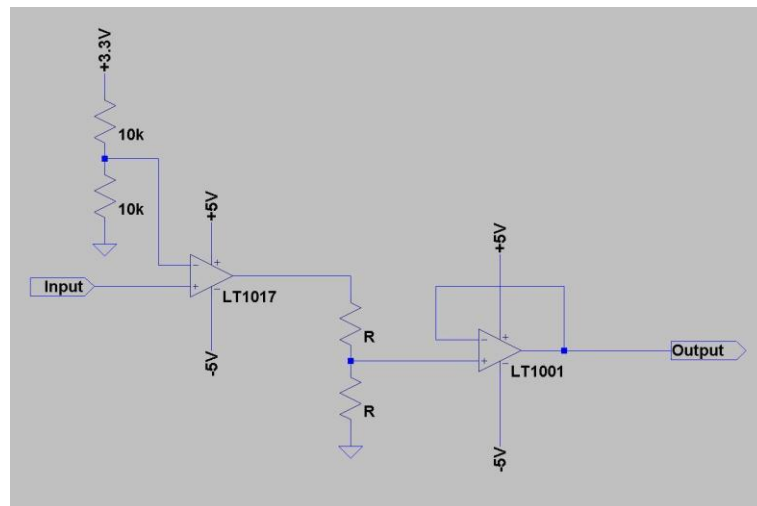


Figure 4.1 - Level shifter circuit

The output of the level shifter was connected to the input of the power amplifier. Research was conducted to determine whether to design and build a power amplifier or to purchase a power amplifier. A company was found, Power Amp Design, that manufactured high voltage, high power op amps suitable for use in driving piezoelectric transducers. The PAD113 high voltage op amp was ideally suited to provide the voltage and current levels needed to drive the transducers. Specifically, the PAD113 op amp featured output voltage capabilities to  $\pm 240$  V, current sourcing capability to 1.5 A, and output power capabilities to 97 W. The PAD113 was designed as a single 2 inch square printed circuit board with integrated heat sink and cooling fan. An adapter printed circuit board was included with the op amp to facilitate connections to and from the op amp.

Configuring the op amp was simple with the help of the PAD113 datasheet [9]. A simple inverting amplifier was configured with the addition of a capacitance which was used to provide phase compensation and slew rate adjustment. The op amp was configured to provide a gain of 100 and a slew rate of up to 40 V/ $\mu$ s. A schematic of the amplifier circuit is given in Figure 4.2. A picture of the op amp is given in Figure 4.3.

The final element required for the driving circuit was a dual-polarity power supply in which to use to power the op amp. A Vicor model VI-PUBB-EYY dual  $\pm 95$  V<sub>DC</sub>, 50 W output AC-DC power supply was used to provide the  $\pm 95$  V<sub>DC</sub> needed to drive the transducers. Using information given in the Vicor datasheet [10], the two outputs of the power supply were connected and 1N4005 diodes were used as steering diodes to prevent one output from back-driving the other output. Figure 4.4 shows the configuration of the power supply to generate  $\pm 95$  V<sub>DC</sub>.

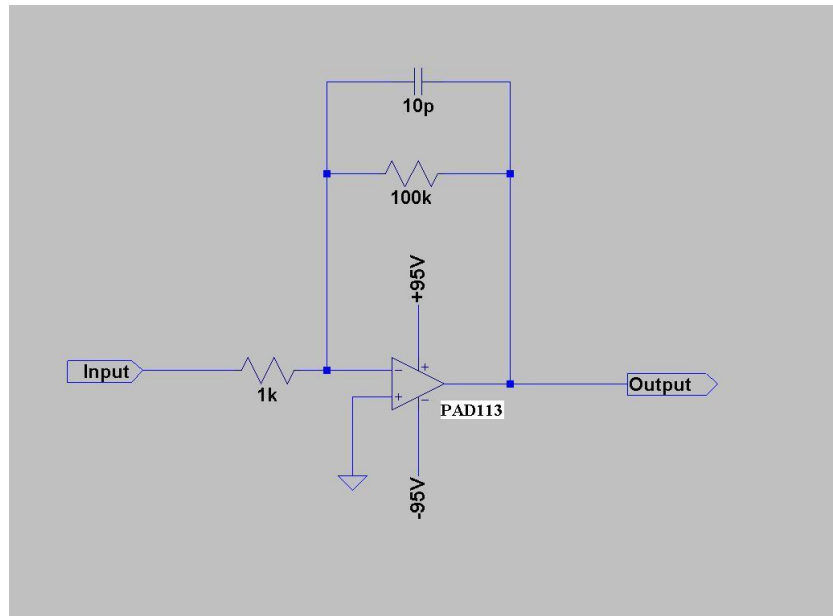


Figure 4.2 - PAD113 op amp circuit

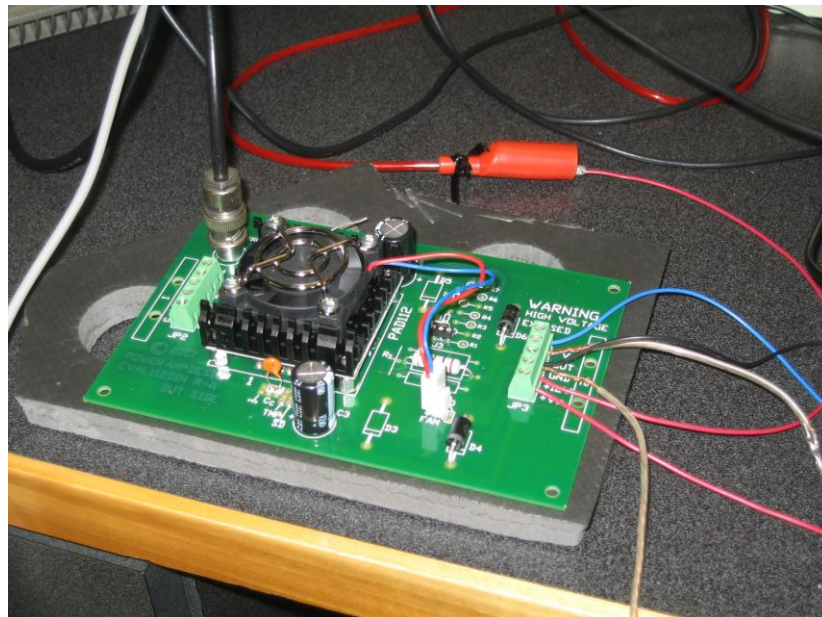


Figure 4.3 - PAD113 power op amp



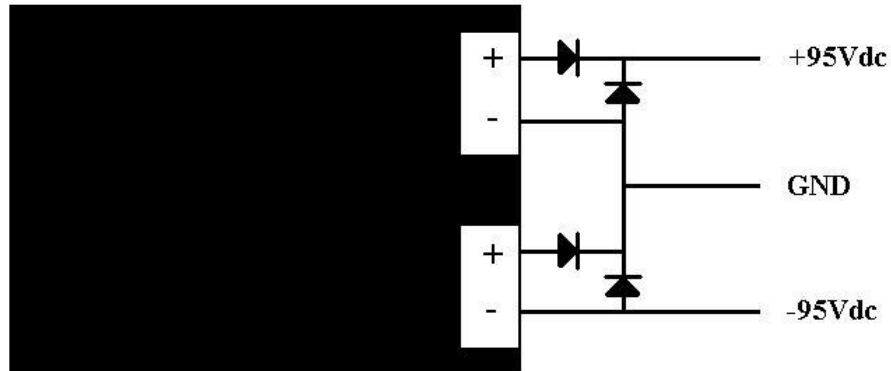


Figure 4.4 -  $\pm 95$  power supply output wiring schematic

In addition to the  $\pm 95$  V<sub>DC</sub> AC-DC power supply, a +12 V<sub>DC</sub> AC-DC power supply was utilized in order to provide power to the PAD113 cooling fan and to provide a power source for the level shifter and microcontroller circuitry which utilized voltage regulators to produce the  $\pm 5$  V<sub>DC</sub> and 3.3 V<sub>DC</sub> respectively needed to supply those circuits.

As mentioned earlier in this chapter, a GUI was developed to allow the driving frequency of the microcontroller to be changed if needed. The GUI was written in Tcl/Tk using information from the Tcl Developer Xchange [11], and provided a front end to the UART communication interface between the host PC and the microcontroller. As noted previously, the microcontroller operates at the default rate of 47.7 kHz upon power-up with no host PC intervention. If alteration of the driving signal frequency was needed, the user would issue the command to place the microcontroller in the proper operating frequency, and operation would continue at that frequency thereafter. A screenshot of the

GUI is shown in Figure 4.5, and the code listing for the GUI is given in Appendix 2.

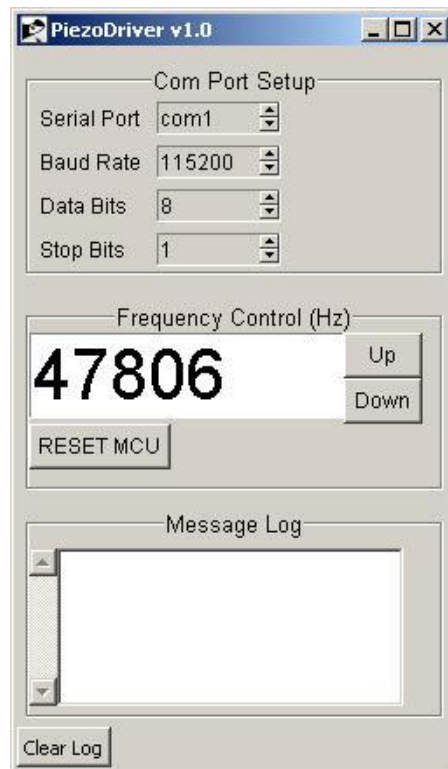


Figure 4.5 - GUI

## 4.2 Receiving Circuit

The receiving circuit was a simple design consisting of a full-wave rectifier and a DC-DC converter. The full-wave rectifier was constructed using four 1N4005 diodes and a high-voltage electrolytic capacitor to smooth the resulting output DC waveform. The DC-DC converter was an integrated unit that featured high input voltage, up to 40 V<sub>DC</sub>, an output of 5 V<sub>DC</sub>, an operating efficiency of 82%, and an output power capability of 20W. These two circuit elements were all that were needed to meet the requirements of

providing suitable input power for the load electronics. The full-wave rectifier converted the sinusoidal signal of the receiving transducer to a DC signal, and the DC-DC circuit converted the DC level to the appropriate level for use by the load electronics.

## CHAPTER 5

### CONCLUSIONS

The piezoelectric transducer-based power through steel system was a simple solution to a challenging problem; bringing power into an area that was sealed and inaccessible. In lieu of drilling holes to run cable to feed power to the electronic circuit located inside the sealed enclosure, a novel through-steel power transfer system was devised that performed well, used commonly available COTS components, was reliable, and was easy to setup once design and analysis had been performed. The key benefits that this system offered were low cost design and installation, high reliability, and good performance.

Applications using piezoelectric transducers are plentiful, as piezoelectric ceramics have found widespread use due to their dependability, efficiency of operation, low cost, and well-known characteristics. The through-steel power transfer system is well suited for use in applications that require electrical devices to be sealed inside of compartments or enclosures that prohibit the use of wires to be used to power the device. HY100 steel was used as the separating medium through which acoustic signals were transferred in this application. Further research is needed in order to characterize the use of the power transfer system with medium other than steel, such as plastic and glass, as new uses for the technology could emerge.

Future work is needed to discover answers for several challenges that arose during the progression of work on the through-steel power transfer system. Of particular interest

is a phenomenon that was noticed when the through-steel power transfer system was tested one year after initial testing had been performed. Using the same test equipment and test parameters that were used in the initial testing, lower power transfer efficiencies were observed. The tests were performed several times to make certain of the differences between the two sets of tests. The new tests consistently resulted in power transfer efficiencies of about 57%, which was 12% lower than those measured one year prior. One explanation of the difference could be found through analysis of the epoxy used to bond the transducers to the steel plate. During aging, the epoxy could become more brittle and less elastic, therefore hampering power transfer by restricting synergistic movement between the transducers and the steel plate. Further work is needed to provide better understanding of the effects that epoxy has on the through-steel power transfer system. Continuation on the works of Prassianakis et al. [12], Perepechko et al. [13], and Lindrose [14] is needed to characterize the acoustic velocity of cured epoxy and to analyze the effect that epoxy has on ultrasonic signal attenuation.

Of additional interest for further research is that of the signal used to excite the driving transducer. In this work, both sinusoidal and square wave periodic signals were used successfully to achieve power transfer. When driving the system with a square wave signal, the resulting output signal would always be a sinusoidal wave, indicating that the additional power in the edges of the square wave driving signal were being lost or wasted. Given that sinusoidal and square wave input signals produced similar output power levels, using a sinusoidal input signal should result in greater overall power efficiency since no signal edges would be lost during the transfer process. Furthermore, a

sinusoidal signal produces none of the harmonics present in a square wave signal, minimizing the likelihood that the through-steel power transfer system would cause interference with other electronic or mechanical systems.

One last point of interest is the attenuation of the transmitted signal in the HY100 steel plate. The third transducer was mounted to the steel plate in an offset position to the driving/receiving transducer pair. Some cursory measurements were taken to observe the amount of signal attenuation at the offset position on the steel plate. The signal attenuation was sufficiently great as to not be problematic for this application. No additional analysis was performed with this offset transducer. Additional analysis is needed to ascertain the level of attenuation in HY100 steel at the operating point of the power through steel transfer system to provide a baseline for future applications that may be sensitive to the level of vibration in the power transfer system. This analysis would also serve to offer a tolerance factor for the alignment of the driving/receiving transducer pair, which is one of the most crucial aspects of the power transfer system.

The power through steel piezoelectric transducer-based transfer system worked ideally for the application described in this thesis, and presented a novel, yet practical, way to solve a unique challenge. Further work could yield new applications for the technology and provide better understanding of its operation. A better understanding of the operation of the through-steel power transfer system could result in a realization of specialized, or at least more ideal, components that could result in greater power transfer efficiencies.

## REFERENCES

- [1] Penella, M.T.; Gasulla, M.; “A Review of Commercial Energy Harvesters for Autonomous Sensors,” Proceedings of IMTC 2007, pp. 1-5, May 2007.
- [2] Hu, Y.; Zhang, X.; Yang, J.; Jiang, Q.; “Transmitting electric energy through a metal wall by acoustic waves using piezoelectric transducers,” in IEEE Transactions on Ultrasonics, Ferroelectrics, and Frequency Control, Volume: 50 , Issue: 7, Digital Object Identifier: 10.1109/TUFFC.2003.1214497 Publication Year: 2003 , Page(s): 773 – 781
- [3] Agilent Technologies, Inc. *Agilent 33220A User’s Guide* [Online]. Available: <http://www.agilent.com>
- [4] APC International Ltd., *Piezoelectric Ceramics: Principles and Applications*. Mackeyville, PA: APC International Ltd., 2002.
- [5] Silicon Laboratories. (2005, December). *C8051F120/1/2/3/4/5/6/7 C8051F130/1/2/3 Mixed Signal ISP Flash MCU Family* [Online]. Available: <http://www.silabs.com>
- [6] Keil. (2004). *μVision User’s Guide* [Online]. Available : <http://www.keil.com/support/man/docs/uv3/>
- [7] Linear Technology Corporation. (2008). *LT1017 / LT1018 Micropower Dual Comparator* [Online]. Available: <http://www.linear.com>
- [8] Linear Technology Corporation. (1983). *LT1001 Precision Operational Amplifier* [Online]. Available: <http://www.linear.com>
- [9] Power Amp Design. *High Voltage Operational Amplifier PAD113 Rev H* [Online]. Available: <http://www.powerampdesign.net>

- [10] Vicor Corporation. *Data Sheet FlatPAC 50 to 600 Watts Autoranging AC-DC Switchers* [Online]. Available: <http://www.vicr.com>
- [11] ActiveState. *Tcl Developer Xchange* [Online]. Available: <http://www.tcl.tk>
- [12] Prassianakis, J.N.; Kompoti, N.; Varakis, J.; “Curing Effects on the Acoustical Properties of Epoxy Polymers,” *Experimental Mechanics*, pp. 77-80, March 1993.
- [13] Perepechko, I.I.; Danilov, V.A.; Nizhegorodov, V.V.; “Ultrasonic Velocity in Epoxy Resin at Temperatures down to 4.2 K\*,” *Mechanics of Composite Materials*, vol. 32, no. 4, pp. 316-320, July, 1996.
- [14] Lindrose, A.M.; “Ultrasonic Wave and Moduli Changes in a Curing Epoxy Resin,” *Experimental Mechanics*, pp. 227-232, June 1978.



## APPENDIX 1

### SILICON LABORATORIES C8051F120 CODE LISTING

```
//*****  
// Matt Hobson  
// piezo_controller.c  
// Used to generate the square-wave signal needed to drive the piezoelectric  
// transducer in the through-steel power transfer system. Output Frequency  
// can be altered from default (47.8kHz) via UART commands. PiezoDriver.tcl  
// is designed to interface with this code.  
// Compiled with Keil uVision 3.  
//*****  
  
//*****  
// INCLUDES  
//*****  
  
#include <c8051f120.h>  
  
//*****  
// COMPILER SWITCH OPTIONS FOR BOARD SELECTION  
//*****  
  
#define Eval_Board  
  
//*****  
// SYSTEM CLOCK SELECTION  
// Selects the correct System Clock frequency based on the board in use  
//*****  
  
#ifdef Eval_Board  
#define SYSCLK 22118400  
#endif  
  
//*****  
// Global CONSTANTS  
//*****  
  
sbit LED = P1^6;           // Green LED: '1' = ON; '0' = OFF  
sbit Button = P3^7;        // Pushbutton on Eval board - N.O.  
extern bit rx0;            // Status bit for received data  
extern unsigned char r0;    // Buffer to hold Tx/Rx data  
  
//*****  
// 16 BIT SFR REGISTERS FOR F120  
//*****  
  
sfr16 RCAP2    = 0xCA;     // Timer2 capture/reload  
  
//*****  
// Function PROTOTYPES  
//*****  
  
extern void tx_pc (unsigned char txpc_info); // Function to send data to PC  
extern void enter (void);                   // CR & LF from UART0  
void Init_Device(void);                     // Device configuration  
void Timer_Init(void);                     // Timer initialization  
void UART_Init(void);                      // UART initialization  
void Voltage_Reference_Init(void);          // Voltage Ref initialization
```

```

void Port_IO_Init(void);           // Port I/O initialization
void Oscillator_Init(void);       // Oscillator initialization
void Interrupts_Init(void);       // UART Interrupt initialization

//*****
// MAIN Routine
//*****

void main (void)
{
    bit n = 0;                     // Status bit
    bit m = 0;                     // Counter

    WDTCN = 0xde;                  // Disable watchdog timer
    WDTCN = 0xad;
    LED = 0;                       // Turn off on-board LED

    Init_Device();                 // Initialize peripherals

    EA = 1;                        // Enable global interrupts

    SFRPAGE = LEGACY_PAGE;         // Page to sit in for now

    tx_pc(0x52); tx_pc(0x45); tx_pc(0x41); // Transmit "READY" to terminal
    tx_pc(0x44); tx_pc(0x59); enter();

    while (1)                      // Spin forever
    {
        if(rx0 == 1)               // If data has been received from PC UART
        {
            switch(r0)              // Determine which character was received
            {
                case 'U': RCAP2++; break; //Increment Timer2, Increase Frequency
                case 'D': RCAP2--; break; //Decrement Timer2, Decrease Frequency
                case 'R': WDTCN = 0xA5; break; //Reset the MCU
            }
            rx0 = 0;                // Reset Rx0 buffer
        }
    }

//*****
// INIT_DEVICE
//*****

void Init_Device(void)
{
    Timer_Init();
    UART_Init();
    Voltage_Reference_Init();
    Port_IO_Init();
    Oscillator_Init();
    Interrupts_Init();
}

//*****
// TIMER_INIT
//*****

void Timer_Init()
{
    SFRPAGE = TMR4_PAGE; //Config Timer 4 to get 115.2 kbps for UART0
    TMR4CN = 0x04;
    TMR4CF = 0x08;
    RCAP4L = 0xCA;
    RCAP4H = 0xFF;
    SFRPAGE = TMR2_PAGE; //Config Timer 2 for 47.8kHz squarewave output

```

```

    TMR2CN    = 0x04;
    TMR2CF    = 0x0A;
    RCAP2L    = 0xEF;
    RCAP2H    = 0xFB;
}

//*****
// UART_INIT
//*****

void UART_Init()
{
    SFRPAGE    = UART0_PAGE;
    SCON0      = 0x50;          //UART0 8-bit variable rate, enable receiver
    SSTA0      = 0x0F;          //UART0 Tx & Rx clocks from Timer 4
}

//*****
// VOLTAGE_REFERENCE_INIT
//*****

void Voltage_Reference_Init()
{
    SFRPAGE    = ADC0_PAGE;      //Enable Temp. Sensor
    REFOCN     = 0x04;
}

//*****
// PORT_IO_INIT
//*****

void Port_IO_Init()
{
    // P0.0 - TX0 (UART0), Push-Pull, Digital
    // P0.1 - RX0 (UART0), Open-Drain, Digital
    // P0.6 - T2 (Timer2), Push-Pull, Digital
    // All Others - Unassigned, Open-Drain, Digital

    SFRPAGE    = CONFIG_PAGE;
    POMDOUT    = 0x41;
    P1MDOUT    = 0x40;
    XBR0       = 0x06;
    XBR1       = 0x20;
    XBR2       = 0xC0;
}

//*****
// OSCILLATOR_INIT
//*****

void Oscillator_Init()
{
    int i = 0;
    SFRPAGE    = CONFIG_PAGE;
    OSCXCN     = 0x67;
    for (i = 0; i < 3000; i++); // Wait 1ms for initialization
    while ((OSCXCN & 0x80) == 0);
    PLL0CN     = 0x04;
    CCH0CN     &= ~0x20;
    SFRPAGE    = LEGACY_PAGE;
    FLSCl      = 0xB0;
    SFRPAGE    = CONFIG_PAGE;
    CCH0CN     |= 0x20;
    PLL0CN     |= 0x01;
    PLL0DIV    = 0x04;
    PLL0FLT    = 0x0F;
    PLL0MUL    = 0x12;
}

```

```

        for (i = 0; i < 15; i++); // Wait 5us for initialization
        PLL0CN |= 0x02;
        while ((PLL0CN & 0x10) == 0);
        CLKSEL = 0x02;
        OSCICN &= ~0x80;
    }

//*****
// INTERRUPTS_INIT
//*****

void Interrupts_Init()
{
    IE      = 0x10;          //Enable interrupts for UART0
    IP      = 0x10;          //UART0 Interrupts set to high priority
}

//*****
// END OF FILE
//*****

//*****
// Matt Hobson
// uart0.c
// Basic Functionality for SiLABS C8051F120 UART
// SiLABS C8051F120
//*****

//*****
// FUNCTION PROTOTYPES
//*****

void tx_pc (unsigned char txpc_info); // Function to send data to PC
void rx_pc (unsigned char);           // Function to receive data from PC
void enter (void);                    // CR & LF from UART0 to PC terminal
void uart0_isr(void);                 // Interrupt Service Routine - UART0

//*****
// VARIABLES
//*****

unsigned char t[] = 0; // Array buffer to hold Tx data
unsigned char r0;      // Buffer to hold Rx data
unsigned int a = 0;     // Counter variable
unsigned char b = 0;    // Counter variable
bit rx0 = 0;           // Status bit for received data
bit ready = 0;          // Status bit for Tx/Rx
bit stopped = 1;        // Status bit for Tx/Rx

//*****
// DEFINES
//*****

#define UART0

//*****
// FUNCTION TX_PC ()
//*****

void tx_pc (unsigned char txpc_info)
{
    while((TI0 == 1) || ((SSTA0 & 0x20) == 0x20)) // Wait for flags to clear
    {;}
    SBUF0 = txpc_info; // Transmit Info to PC
    for(a=0;a<5000;a++) // Transmission delay

```

```

    {;}
}

//*****
// FUNCTION ENTER ()
// Outputs a carriage return and a line feed from UART0 to the PC terminal
//*****

void enter (void)
{
    tx_pc(0xD);    // Carriage Return
    tx_pc(0xA);    // New Line
}

//*****
// INTERRUPT SERVICE ROUTINE: UART0_ISR ()
//*****

void uart0_isr (void) interrupt 4
{
    if(TI0 == 1)
    {
        TI0 = 0;    // Clear Tx Flag
    }
    if(RI0 == 1)
    {
        r0 = SBUF0;    // Store Received Data
        rx0 = 1;    // Set receive bit
        RI0 = 0;    // Clear Rx Flag
    }
}

//*****
// INTERRUPT SERVICE ROUTINE: UART1_ISR ()
//*****

#ifdef UART1
void uart1_isr (void) interrupt 20
{
    if(TI1 == 1)
    {
        TI1 = 0;    // Clear Tx Flag
    }
    if(RI1 == 1)
    {
        r1 = SBUF0;    // Store Received Data
        rx1 = 1;    // Set receive bit
        RI1 = 0;    // Clear Rx Flag
    }
}
#endif

//*****
// END OF FILE
//*****

```

## APPENDIX 2

### TCL/TK GUI CODE LISTING

```
# v1.0 20080623, PMH, Written for tcl 8.5 or later

#####
#
#####

wm title . "PiezoDriver v1.0"

#####
# Create Main Frames
#####

frame .left
grid .left \
    -sticky nwes

#####
# Fill in the Serial Port Frame
#####

labelframe .left.portFrame \
    -font "universobl 10" \
    -labelanchor n \
    -text "Com Port Setup"
grid .left.portFrame \
    -padx 5 \
    -pady 10 \
    -sticky nwes
set portNumsList [list com1 com2 ]
set baudRatesList [list 115200 2400 4800 9600 19200 38400 57600]
set dataBitsList [list 8 7 6 5 ]
set stopBitsList [list 1 1.5 2 ]
set portOpen 0

label .left.portFrame.portLabel \
    -font "universobl 9" \
    -text "Serial Port"
label .left.portFrame.baudLabel \
    -font "universobl 9" \
    -text "Baud Rate"
label .left.portFrame.dataLabel \
    -font "universobl 9" \
    -text "Data Bits"
label .left.portFrame.stopLabel \
    -font "universobl 9" \
    -text "Stop Bits"
label .left.portFrame.addressLabel \
    -font "universobl 9" \
    -text "Address"

spinbox .left.portFrame.portSpin \
    -values $portNumsList \
    -width 8 \
    -font "universobl 9" \
    -wrap 1 \
    -state readonly \
```

```

        -textvariable portNum
spinbox .left.portFrame.baudSpin \
    -values $baudRatesList \
    -width 8 \
    -font "universobl 9" \
    -wrap 1 \
    -state readonly \
    -textvariable baudRate
spinbox .left.portFrame.dataSpin \
    -values $dataBitsList \
    -width 8 \
    -font "universobl 9" \
    -wrap 1 \
    -state readonly \
    -textvariable dataBits
spinbox .left.portFrame.stopSpin \
    -values $stopBitsList \
    -width 8 \
    -font "universobl 9" \
    -wrap 1 \
    -state readonly \
    -textvariable stopBits

grid .left.portFrame.portLabel .left.portFrame.portSpin -sticky w -pady 2 -padx 3
grid .left.portFrame.baudLabel .left.portFrame.baudSpin -sticky w -pady 2 -padx 3
grid .left.portFrame.dataLabel .left.portFrame.dataSpin -sticky w -pady 2 -padx 3
grid .left.portFrame.stopLabel .left.portFrame.stopSpin -sticky w -pady 2 -padx 3

#####
# Fill in the Control Frame                                     #
#####

labelframe .left.ctrlFrame \
    -font "universobl 10" \
    -labelanchor n \
    -text "Frequency Control (Hz)"
grid .left.ctrlFrame \
    -pady 5 \
    -padx 5 \
    -ipady 5 \
    -ipadx 5 \
    -sticky ew

#####
# Data Rate %                                                 #
#####

entry .left.ctrlFrame.freqEnt \
    -font "universobl 30" \
    -textvariable freq \
    -relief sunken \
    -width 8 \
    -justify left
set RCAP2 64495
set freq [expr (99532800 / (2*(65536 - $RCAP2)))]
button .left.ctrlFrame.freqUp \
    -font "universobl 9" \
    -text "Up" \
    -width 5 \
    -command setFreqUp
button .left.ctrlFrame.freqDown \
    -font "universobl 9" \
    -text "Down" \
    -width 5 \
    -command setFreqDown
button .left.ctrlFrame.reset \
    -font "universobl 9" \

```

```

        -text "RESET MCU" \
        -command reset

#####
# WIDGET ALIGNMENT
#####

grid .left.ctrlFrame \
    -pady 5 \
    -sticky nw
grid configure .left.ctrlFrame.freqEnt -rowspan 2 -row 5 -columnspan 2 -column 0 -sticky
nw
grid configure .left.ctrlFrame.freqUp -row 5 -column 2 -sticky nw
grid configure .left.ctrlFrame.freqDown -row 6 -column 2 -sticky nw
grid configure .left.ctrlFrame.reset -row 7 -column 0 -sticky nw

#####
# Fill in the Log View Frame
#####

labelframe .left.logFrame \
    -text "Message Log" \
    -font "universobl 10" \
    -labelanchor n
grid .left.logFrame \
    -sticky nwse \
    -columnspan 2 \
    -pady 5 \
    -padx 5
set log [text .left.logFrame.log \
    -width 32 \
    -height 6 \
    -font "universobl 8" \
    -borderwidth 2 \
    -relief sunken \
    -setgrid true \
    -yscrollcommand {.left.logFrame.scroll set}]
scrollbar .left.logFrame.scroll \
    -command {.left.logFrame.log yview}
grid .left.logFrame.scroll .left.logFrame.log \
    -pady 5 \
    -sticky nsw
frame .left.buttonFrame
grid .left.buttonFrame \
    -sticky nwe \
    -columnspan 2
checkboxbutton .left.buttonFrame.verboseMode \
    -text "VERBOSE MODE" \
    -variable verboseMode
button .left.buttonFrame.clearButton \
    -text "Clear Log" \
    -command clearLog
grid .left.buttonFrame.clearButton \
    -sticky nwe

#####
# Procedures
#####

#after 500 comRd 5

#####
# COMMAND: FREQUENCY UP
#####

proc setFreqUp { } {

```



```

global freq \
        RCAP2 \

set RCAP2 [expr {$RCAP2 + 1}]
set freq [expr (99532800 / (2*(65536 - $RCAP2)))]
set comStr [binary format c 0x55]
comWrt $comStr
#closePort
logWrt ">> Frequency Increased\n"
}

#####
# COMMAND: FREQUENCY DOWN #
#####

proc setFreqDown { } {
    global freq \
            RCAP2

    set RCAP2 [expr {$RCAP2 - 1}]
    set freq [expr (99532800 / (2*(65536 - $RCAP2)))]
    set comStr [binary format c 0x44]
    comWrt $comStr
    #closePort
    logWrt ">> Frequency Decreased\n"
}

#####
# COMMAND: RESET #
#####

proc reset { } {
    global freq \
            RCAP2
    set RCAP2 64495
    set freq [expr (99532800 / (2*(65536 - $RCAP2)))]
    set comStr [binary format c 0x52]
    comWrt $comStr
    #closePort
    logWrt ">> System Reset\n"
}

#####
#COMMAND: SERIAL PORT WRITE #
#####

proc comWrt { comStr } {
    global portID \
            portOpen \
            verboseMode

    if { $portOpen == 0 } {
        if { [openPort] == -1 } {
            logWrt "Error opening port\n"
            return -1
        }
        after 100
    }
    flush $portID

    if { $verboseMode == 1 } {
        logWrt "Writing $comStr\n"
    }

    if { [catch { puts -nonewline $portID $comStr } result ] } {
        logWrt "Error reading from port $portID, Error: $result\n"
    }
}

```

```

        #closePort
        return -1
    } else {
        flush $portID
        return 0
    }
}

#####
#COMMAND: SERIAL PORT READ
#####

proc comRd { numBytes } {
    global portID \
           portOpen \
           verboseMode

    if { $portOpen == 0 } {
        if { [openPort] == -1 } {
            logWrt "Error opening port\n"
            return -1
        }
    }

    if { [catch { read $portID $numBytes } result] } {
        logWrt "Error reading from port $portID, Error: $result\n"
        #closePort
        return -1
    } else {
        set rxline $result
        if {$verboseMode == 1} {
            logWrt "Read $rxline\n"
        }
        #return $rxline
    }

    if {$rxline != 0} {
        set RCAP2 64495
        set freq [expr (99532800 / (2*(65536 - $RCAP2)))]
        logWrt "System Reset\n"
    }
}

#####
#COMMAND: MESSAGE LOG WRITE
#####

proc logWrt { logStr } {
    global log
    $log insert end $logStr
    .left.logFrame.log yview moveto 1.0
    update
}

#####
#COMMAND: CLEAR LOG
#####

proc clearLog { } {
    global log
    $log delete 1.0 end
    update
}

#####
#COMMAND: OPEN SERIAL PORT
#####

```

```

proc openPort { } {
    global portNum \
           baudRate \
           dataBits \
           stopBits \
           portID \
           portOpen \
           verboseMode

    if { [catch { open $portNum RDWR } result ] } {
        logWrt "Error opening port $portNum, Error: $result\n"
        set portOpen 0
        return -1
    } else {
        set portID $result
        set portOpen 1

        fconfigure $portID \
            -mode $baudRate,n,$dataBits,$stopBits \
            -blocking 1 \
            -buffersize 300 \
            -buffering full \
            -handshake none \
            -translation { binary binary }

        if {$verboseMode == 1} {
            logWrt "COM Port Opened\n"
        }

        return 0
    }
}

#####
#COMMAND: CLOSE SERIAL PORT      #
#####

proc closePort { } {
    global portID \
           portOpen \
           verboseMode

    if { $portOpen == 1 } {
        close $portID
        if {$verboseMode == 1} {
            logWrt "COM Port closed\n"
        }
        set portOpen 0
    }
}

#####
# END                             #
#####

```